Iridium Alkoxide and Amide Hydride Complexes. Synthesis, Reactivity, and the Mechanism of O–H and N–H Reductive Elimination

David S. Glueck, Linda J. Newman Winslow, and Robert G. Bergman*

Department of Chemistry, University of California, Berkeley, California 94720

Received October 29, 1990

The ethoxy hydride complex Cp*IrPPh$_3$(OEt)(H) (**3**, Cp* = η^5-C$_5$Me$_5$) was prepared from Cp*IrPPh$_3$Cl$_2$ and sodium ethoxide in ethanol. Ethoxide **3** reacted with alcohols to form the alkoxy hydrides Cp*IrPPh$_3$(OR)(H) (R = OCD$_2$CD$_3$, **6a**; R = *n*-Pr, **6b**; R = *i*-Pr; **6c**; R = Ph, **6e**) and with amines to give the amido hydrides Cp*IrPPh$_3$(NHR)(H) (R = Ph, **8a**; R = CH$_2$Ph, **8b**). The isopropoxide **6c** was characterized by X-ray diffraction ($P2_1/c$; a = 11.7943 (13) Å, b = 11.7467 (8) Å, c = 20.3034 (27) Å, β = 96.56 (1)°, V = 2794.5 (9) Å^3, 3642 unique data, 2979 for which $F^2 > 3\sigma(F^2)$; R = 1.59%, R_w = 2.08%, GOF = 1.378). Irradiation of complex **3** yielded ethanol and the phosphine-cyclometalated complex Cp*Ir(PPh$_2$C$_6$H$_4$)(H) (**5a**) in cyclooctane or a mixture of **5a** and Cp*IrPPh$_3$(Ph)(H) (**5b**) in benzene. The reaction of **3** with heterocumulenes afforded the products of insertion into the Ir–O bond, Cp*IrPPh$_3$(OCO$_2$Et)(H) (**9**), Cp*IrPPh$_3$(S$_2$COEt) (**10**), and Cp*IrPPh$_3$(RNCO$_2$Et) (R = Ph, **11a**; R = *p*-Tol, **11b**; R = Me, **11c**). Similarly, CS$_2$ underwent insertion into the Ir–N bond of the amido hydrides **8a,b** to form Cp*IrPPh$_3$(S$_2$CNHR)(H) (R = Ph, **12a**; R = CH$_2$Ph, **12b**). Reaction of MeNCO with **8a**, however, gave Cp*IrPPh$_3$(NPhC(O)NHMe)(H) (**13b**). The reaction of **3** with several two-electron donor ligands yielded ethanol and the Ir(I) compounds Cp*IrPPh$_3$(L) (L = CO, **14**; L = C$_2$H$_4$, **15**; L = CN-*t*-Bu, **16**; L = PPh$_3$, **17**; L = PPh$_2$Me, **18**). The anilido hydride **8a** underwent similar elimination reactions with these ligands to afford **14–18** and aniline; benzylamido hydride **8b** reacted with PPh$_3$ to give benzylamine and **17**. Saturation kinetics were observed in all cases for the reaction of PPh$_3$ with **3** and **8a,b** in toluene, suggesting that these alkoxy and amido hydride compounds reversibly form an intermediate that is trapped by PPh$_3$ to form **17** and alcohol or amine. Additional evidence is provided that supports the ring-slipped species (η^3-C$_5$Me$_5$)IrPPh$_3$(X)(H) (X = OEt, NHPh, NHCH$_2$Ph) as the identity of this intermediate.

Introduction

The metal–carbon bond has by definition been the traditional focus of organometallic chemistry. Rational syntheses of metal alkyl complexes are now available; such fundamental processes as oxidative addition, reductive elimination, and migratory insertion have been extensively studied. Many homogeneous catalytic reactions that result in C–H or C–C bond formation proceed by combinations of such organometallic reactions.[1] Similarly, fundamental information on the preparation and reactivity of metal alkoxide and amide complexes is required to develop and understand catalytic processes resulting in the formation of H–heteroatom (O or N) and C–heteroatom bonds.

Alkoxy and amide coordination complexes and organometallic compounds of the early transition metals are well-known.[2] These species often contain robust M–O and M–N bonds, perhaps because of a favorable donor–acceptor interaction between the heteroatom lone pair and an empty orbital of the metal.[2] Bonds between low-valent late transition metals and O or N are less common; it has been proposed that the interaction between the hard ligand and the soft late metal is unfavorable and leads to weak metal–heteroatom bonds.[4] Studies of these complexes have also been hampered by their facile decomposition to metal hydrides by β-elimination pathways. Indeed β-elimination of metal alkoxides is a classical route to hydrides.[3] Recently, however, several stable late-transition-metal alkoxide and amide complexes have been synthesized and their reactivity investigated;[4] still, mechanistic information is sparse.

We report here the preparation of η^5-pentamethylcyclopentadienyl (Cp*) hydride complexes of iridium containing alkoxide and amide ligands, their reactivity, and mechanistic studies of their reductive elimination and insertion reactions.[5] These compounds, of the form Cp*IrPPh$_3$(H)(X) where X = OR or NHR, enable direct comparison of the Ir–O and Ir–N bonds to the corresponding Ir–C and Ir–H bonds in the complexes Cp*IrPR'$_3$(R)(H) (R' = Me, Ph), which have been extensively studied in our work on C–H activation of alkanes.[6]

A few recent mechanistic studies have been carried out on late-metal alkoxide insertion reactions; almost nothing is known as yet about the mechanism of reactions of the late-transition-metal–amide bond. The alkoxide investigations have focused largely on coordinatively unsaturated, square-planar d^8 complexes. Atwood et al.[7a] investigated the Vaska-type complexes (PPh$_3$)$_2$Ir(CO)OR while Bryndza[7b,c] examined (dppe)Pt(Me)OR. In each case, the initial step of the insertions was postulated to involve coordination of a ligand at the vacant site. We expected that the coordinatively saturated iridium systems considered in this work might react by different pathways.

Results and Discussion

Synthesis of Iridium Alkoxide Hydrides. Metathesis of metal halides with alkali-metal alkoxides is a classical route to metal alkoxides,[8] but in organometallic chemistry

(1) Collman, J. P.; Hegedus, L. S.; Norton, J. R.; Finke, R. G. *Principles and Applications of Organotransition Metal Chemistry*; University Science Books: Mill Valley, CA, 1987; pp 279–669.
(2) (a) Bradley, D. C.; Mehrotra, R. C.; Gaur, D. P. *Metal Alkoxides*; Academic Press: New York, 1978. (b) Lappert, M. F.; Power, P. P.; Sanger, A. R.; Srivastava, R. C. *Metal and Metalloid Amides*; Ellis Horwood: Chichester, U.K., 1980.
(3) Chatt, J.; Shaw, B. L. *J. Chem. Soc.* **1962**, 5075.
(4) Recent reviews: (a) Alkoxides and amides: Bryndza, H.; Tam, W. *Chem. Rev.* **1988**, *88*, 1163. (b) Amides: Fryzuk, M. D.; Montgomery, C. D. *Coord. Chem. Rev.* **1989**, *95*, 1.
(5) Synthesis of the alkoxy hydrides has been published in preliminary form: Newman, L. J.; Bergman, R. G. *J. Am. Chem. Soc.* **1985**, *107*, 5314.
(6) Bergman, R. G. *Science* **1984**, *223*, 902.
(7) (a) Rees, W. M.; Churchill, M. R.; Fettinger, J. C.; Atwood, J. D. *Organometallics* **1985**, *4*, 2179. (b) Bryndza, H. E. *Organometallics* **1985**, *4*, 1686. (c) Bryndza, H. E. *Organometallics* **1985**, *4*, 406.
(8) Reference 2a, pp 13–27.

0276-7333/91/2310-1462$02.50/0

Scheme I

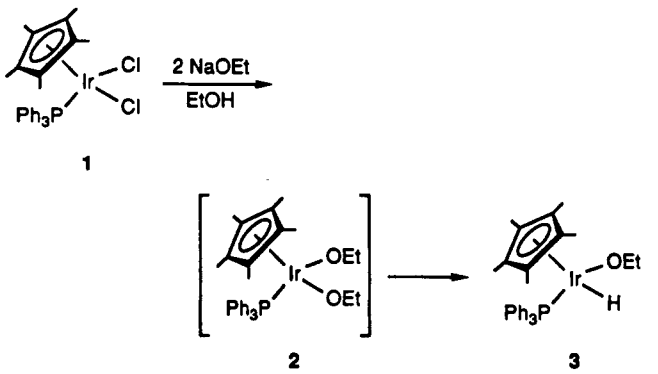

this method often leads to hydrides.[3] Treatment of an orange slurry of $Cp^*IrPPh_3Cl_2$ (1) in ethanol with greater than 2 equiv of sodium ethoxide gives a homogeneous yellow solution from which yellow crystals can be isolated in high yield. The product of this reaction is neither the simple metathesis product $Cp^*IrPPh_3(OEt)_2$ (2) nor the dihydride $Cp^*IrPPh_3H_2$ but the ethoxy hydride $Cp^*IrPPh_3(OEt)(H)$ (3) (Scheme I). In the ^1H NMR spectrum of 3, the ethoxide protons appear as an $AA'B_3$ pattern. The diastereotopic methylene protons give rise to a doublet of multiplets at δ 3.79 (C_6D_6) with ^2J = 9.0 Hz and ^3J = 6.0 Hz. The methyl protons appear as a triplet with J = 6.0 Hz. In the $^{13}C\{^1H\}$ NMR spectrum, the ethoxide carbon signals appear at δ 75.3 (methylene) and 23.9 (methyl). The iridium hydride is observed by both ^1H NMR (δ −13.20, d, J_{HP} = 37.7 Hz) and IR (2035 cm^{-1}) spectroscopy. $Cp^*IrPMe_3(OEt)(H)$ can be prepared similarly; for experimental convenience we investigated only the more crystalline triphenylphosphine derivative, which was also characterized by elemental analysis and ^{31}P NMR spectroscopy.

The mechanism of formation of 3 was briefly investigated. Direct O—H oxidative addition of ethanol to the coordinatively unsaturated fragment Cp^*IrPR_3 was discounted by irradiating $Cp^*IrPMe_3H_2$ in ethanol. The product of this reaction is the vinyl hydride $Cp^*IrPMe_3(CH{=}CH_2)(H)$,[9] presumably formed by dehydration of the initial C—H activation product $Cp^*IrPMe_3(CH_2CH_2OH)(H)$. This experiment is not conclusive, as 3 is not photostable (see below). However, the absence of the cyclometalated $Cp^*Ir(PPh_2C_6H_4)(H)$ (**5a**)[10a] supports the view that Cp^*IrPPh_3 is not formed. Labeling studies suggest that the hydride ligand in 3 arises by β-elimination of ethoxide; thus treatment of $Cp^*IrPPh_3Cl_2$ with $NaOCD_2CH_3$ in CH_3CD_2OH gives $Cp^*IrPPh_3(OCD_2CH_3)(D)$. Presumably the ethoxy hydride product and acetaldehyde are formed by β-hydride elimination from unobserved $Cp^*IrPPh_3(OEt)_2$ (2). $Cp^*IrPPh_3(Cl)(H)$ (4),[11] formed by β-elimination from $Cp^*IrPPh_3(OEt)(Cl)$, could react with ethoxide to form the observed product but it can be prepared from and is stable in basic ethanol solutions.

Thermal Properties and Photochemistry of 3. The thermal properties and photochemistry of alkoxy hydride complex 3 is significantly different from that of the analogous alkyl hydrides. Heating $Cp^*IrPR_3(R)(H)$ at 130 °C induces reductive elimination of alkane and generates the 16-electron species Cp^*IrPR_3 (or a solvate of this

Scheme II

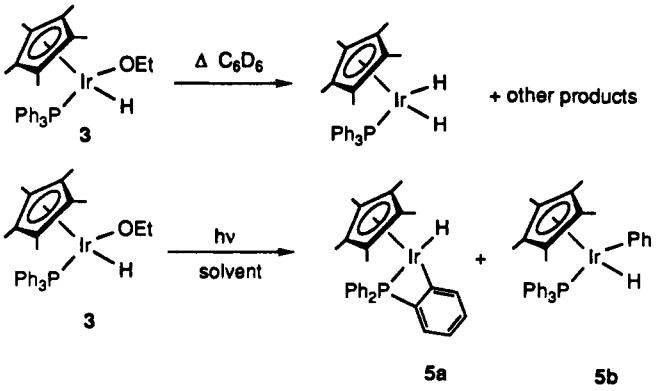

solvent = C_6H_6 **5a**:**5b** ~1:1
solvent = C_8H_{16} only **5a**

Scheme III

6a, R = CD_2CD_3
6b, R = n-Pr
6c, R = i-Pr

"naked" species), which activates the solvent (R = Me)[10,12] or its triphenylphosphine ligand C–H bonds (R = Ph) in competition with those of the solvent.[10] Heating alkoxide 3 in benzene for 30 h at 65 °C, however, leads to a mixture of several products, in which $Cp^*IrPPh_3H_2$[10a] predominates (Scheme II).

The photochemistry of 3 also differs from that of the alkyl hydrides, which are relatively photostable and can be prepared by irradiation of $Cp^*IrPMe_3H_2$ in alkane solvent.[13] Irradiation of 3 causes clean and rapid (minutes) reductive elimination of ethanol and apparent generation of the 16-electron fragment Cp^*IrPPh_3, abbreviated below as [Ir] (see Scheme II). Thus, photolysis of 3 in benzene gives a mixture (~1:1) of the orthometalated complex $Cp^*Ir(PPh_2C_6H_4)(H)$ (**5a**) and the solvent-activation product $Cp^*IrPPh_3(Ph)(H)$ (**5b**). Photolysis in cyclooctane affords only **5a**. These products are identical with those formed on irradiation of the dihydride $Cp^*IrPPh_3H_2$ in Janowicz' initial observations of C–H bond activation.[10]

Preparation of Other Iridium Alkoxide Hydrides. Treatment of ethoxide complex 3 with excess alcohol, either as a neat solution or in an organic cosolvent, gives the new alkoxide complexes $Cp^*IrPPh_3(OR)(H)$ (**6a–c**, R = OCD_2CD_3, O-*n*-Pr, O-*i*-Pr) (Scheme III). Retention of the metal-bound hydride suggests that these reactions do not proceed by a reductive elimination–oxidative addition sequence. Treatment of $[Ir](OCD_2CD_3)(D)$ (3-d_6, prepared from $[Ir]Cl_2$ with $NaOCD_2CD_3$ in $DOCD_2CD_3$ as discussed below) with EtOH gives [Ir](OEt)(D), and dissolving [Ir](OEt)(H) in EtOD does not cause incorporation of D at the hydride position. A similar pathway appears to be operative in other metal alkoxide systems; thus the reaction of $(PMe_3)_4Ir(OH)(H)^+$ with D_2O gives $(PMe_3)_4Ir(OD)(H)^+$.[14]

(9) Stoutland, P. O.; Bergman, R. G. *J. Am. Chem. Soc.* **1988**, *110*, 5732.
(10) (a) Janowicz, A. H. Ph.D. Thesis, University of California Berkeley, 1982. (b) Janowicz, A. H.; Bergman, R. G. *J. Am. Chem. Soc.* **1983**, *105*, 3929.
(11) Moseley, K.; Kang, J. W.; Maitlis, P. M. *J. Chem. Soc. A.* **1970**, 2875.
(12) Buchanan, J. M.; Stryker, J. M.; Bergman, R. G. *J. Am. Chem. Soc.* **1986**, *108*, 1537.
(13) Extended irradiation (days) of the alkyl hydrides $Cp^*IrPMe_3(R)(H)$ in benzene gives $[Ir]H_2$ and then [Ir](Ph)(H). Schade, C.; Bergman, R. G. Unpublished results.

Scheme IV

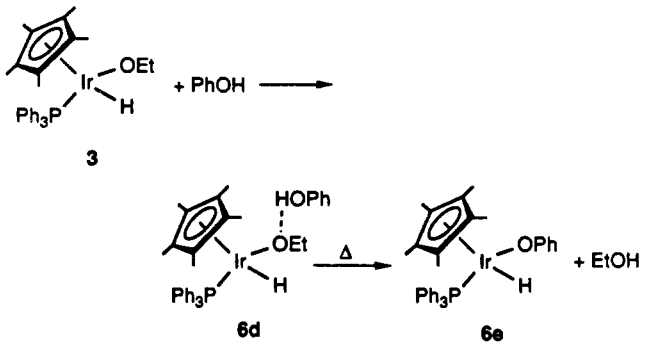

Direct evidence for this mechanism is available from the reaction of **3** with phenol. At room temperature, a number of products are formed, but if phenol is added to **3** as a cold pentane solution and the solvent is immediately removed, the hydrogen-bound phenol adduct $Cp^*IrPPh_3(OEt)(H)\cdot HOPh$ (**6d**) (Scheme IV), sparingly soluble in pentane, can be isolated. The ^1H NMR spectrum of the adduct **6d** shows that the bound phenol remains attached in solution; a signal due to the diastereotopic methylene hydrogens at δ 3.6 suggests that the ethoxide ligand remains bound to iridium. The phenol proton involved in hydrogen bonding appears at δ 11.8, and the metal hydride at δ −12.86 (d, J_{HP} = 37.7). The existence of such hydrogen-bonded adducts in the solid state has been observed earlier; see, for example, the X-ray diffraction study on the complex $Cp^*Rh(O_2C_6H_4)\cdot 2C_6H_4(OH)_2$.[15] However, hydrogen bonds strong enough to maintain the association in solution are more unusual. Recent examples of this phenomenon, supported by both solid-state X-ray and solution NMR studies, include $(PMe_3)_3Rh(O\text{-}p\text{-}Tol\cdot HO\text{-}p\text{-}Tol)$,[16] $PdH(PCy_3)_2(OAr\cdot HOAr)$ (Ar = C_6H_5, C_6F_5),[17] and several Pd and Ni PMe_3 phenoxide complexes.[18] As shown in Scheme IV, heating **6d** in benzene solution completes the hydrogen exchange and leads to the phenoxide $Cp^*IrPPh_3(OPh)(H)$ (**6e**) and ethanol.

Although alkoxy hydride compounds of the early transition metals, such as $Cp_2W(OMe)(H)$[19] and $Cp^*_2Zr(OMe)(H)$[20] were previously known, the $Cp^*(PPh_3)Ir(H)(OR)$ complexes described above were the first isolable low-valent late-transition-metal alkoxy hydride compounds.[5] Earlier, the intermediate $(PMe_3)_4Os(OMe)(H)$[21] was observed by NMR spectroscopy but decomposes to $(PMe_3)_4OsH_2$. $[(PEt_3)_3PtH]^+OEt^-$,[22] in which ethoxide is a counterion, is formed on dissolution of $(PEt_3)_3Pt$ in ethanol. Trogler generated the unstable *trans*-$(PEt_3)_2Pt(OMe)(H)$[23] and recently isolated and crystallographically characterized the phenoxide *trans*-$(PEt_3)_2Pt(OPh)(H)$.[24] The cationic iridium methoxide hydride compound $(PMe_3)_4Ir(OMe)(H)^+$ has also been reported.[25]

Table I. Crystal and Data Collection Parameters for 6c

(A) Crystal Parameters at 25 °C[a,b]

a = 11.7943 (13) Å	cryst size: 0.2 × 0.2 × 0.3 mm
b = 11.7647 (8) Å	space group: $P2_1/c$
c = 20.3034 (27) Å	fw = 649.8
β = 96.56 (1)°	Z = 4
V = 2794.5 (9) Å^3	d_{calc} = 1.54 g cm^{-3}
μ_{calc} = 48.35 cm^{-1}	

(B) Data Measurement Parameters

λ(Mo Kα radiation) = 0.71073 Å
highly oriented graphite monochromator (2θ = 12.2°)
detector: crystal scintillation counter, with PHA
reflns measd: $+h,+k,\pm l$
2θ range: 3–45°
scan type: θ–2θ
scan width: $\Delta\theta = 0.65 + 0.347 \tan\theta$
scan speed: 0.78–6.7°/min (θ)
bckgd: measd over $0.25(\Delta\theta)$ added to each end of the scan
aperture (crystal) = 173 mm
vertical aperture = 3.0 mm
horizontal aperture = 2.2 + 1.0 tan θ mm (variable)
no. of reflns collcd: 4063
no. of unique reflns: 3642
intensity stds: [1,7,−6], (5,3,−12), (7,2,4) (measd every hour of X-ray exposure time)[c]
orientation: three reflns checked after every 250 measurements[d]

[a] Unit cell parameters and their esd's were derived by a least-squares fit to the setting angles of the unresolved Mo Kα components of 24 reflections with 2θ between 27 and 31°. [b] In this and all subsequent tables the esd's of all parameters are given in parentheses, right-justified to the least significant digit(s) given. [c] Over the data collection period a 7% decrease in intensity was observed. [d] Crystal orientation was redetermined if any of the reflections were offset from their predicted positions by more than 0.1°. Reorientation was performed twice during data collection.

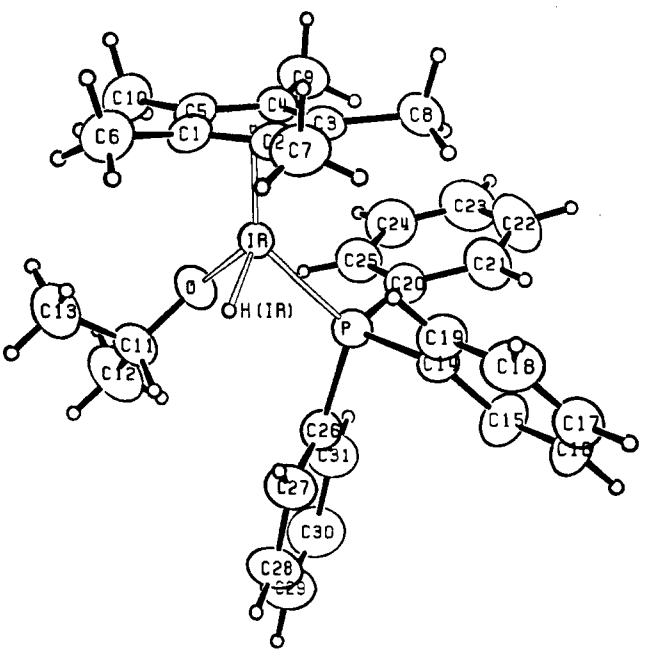

Figure 1. ORTEP diagram for $Cp^*IrPPh_3(O\text{-}i\text{-}Pr)(H)$ (**6c**).

Structure of an Alkoxy Hydride Complex. The structure of complex **6c**, $Cp^*IrPPh_3(O\text{-}i\text{-}Pr)(H)$, was determined by an X-ray diffraction study performed by Dr. Frederick J. Hollander at the UC Berkeley CHEXRAY facility. The compound crystallized in space group $P2_1/c$;

(14) Milstein, D.; Calabrese, J. C.; Williams, I. D. *J. Am. Chem. Soc.* **1986**, *108*, 6387.
(15) Espinet, P.; Bailey, P. M.; Maitlis, P. M. *J. Chem. Soc., Dalton Trans.* **1979**, 1542.
(16) Kegley, S. E.; Schaverien, C. J.; Freudenberger, J. H.; Bergman, R. G.; Nolan, S. P.; Hoff, C. D. *J. Am. Chem. Soc.* **1987**, *109*, 6563.
(17) DiBugno, C.; Pasquali, M.; Leoni, P.; Sabatino, P.; Braga, D. *Inorg. Chem.* **1989**, *28*, 1390.
(18) Kim, Y-J.; Osakada, K.; Takenaka, A.; Yamamoto, A. *J. Am. Chem. Soc.* **1990**, *112*, 1096.
(19) Farrugia, L.; Green, M. L. H. *J. Chem. Soc., Chem. Commun.* **1975**, 416.
(20) Manriquez, J. M.; McAlister, D. R.; Sanner, R. D.; Bercaw, J. E. *J. Am. Chem. Soc.* **1976**, *98*, 6733.
(21) Gotzig, J.; Werner, R.; Werner, H. *J. Organomet. Chem.* **1985**, *285*, 99.
(22) Gerlach, D.; Kane, A. R.; Parshall, G. W.; Jesson, J. P.; Muetterties, E. L. *J. Am. Chem. Soc.* **1971**, *93*, 3543.
(23) Paonessa, R. S.; Prignaro, A. L.; Trogler, W. C. *Organometallics* **1985**, *4*, 647.
(24) Cowan, R. L.; Trogler, W. C. *J. Am. Chem. Soc.* **1989**, *111*, 4730.
(25) Milstein, D.; Calabrese, J. C.; Williams, J. D. *J. Am. Chem. Soc.* **1986**, *108*, 6387.

Table II

(a) Intramolecular Distances (Å)

Ir–P	2.236 (1)	Ir–C3	2.218 (3)
Ir–O	2.076 (2)	Ir–C4	2.272 (3)
Ir–H(Ir)	1.44 (3)	Ir–C5	2.262 (3)
Ir–C1	2.239 (3)	Ir–Cp1	1.880[a]
Ir–C2	2.204 (3)		
O–C11	1.407 (3)	C11–C13	1.506 (5)
C11–C12	1.518 (4)		
C1–C2	1.439 (4)	C1–C6	1.488 (4)
C2–C3	1.432 (4)	C2–C7	1.504 (4)
C3–C4	1.422 (4)	C3–C8	1.498 (4)
C4–C5	1.445 (4)	C4–C9	1.491 (4)
C5–C1	1.413 (4)	C5–C10	1.502 (4)
P–C14	1.821 (3)	P–C26	1.829 (3)
P–C20	1.821 (3)		
C14–C15	1.408 (4)	C22–C23	1.363 (5)
C14–C19	1.364 (4)	C23–C24	1.371 (5)
C15–C16	1.379 (4)	C24–C25	1.372 (4)
C16–C17	1.361 (5)	C26–C27	1.377 (4)
C17–C18	1.370 (5)	C26–C31	1.383 (4)
C18–C19	1.375 (4)	C27–C28	1.391 (4)
C20–C21	1.397 (5)	C28–C29	1.362 (5)
C20–C25	1.387 (4)	C29–C30	1.360 (5)
C21–C22	1.380 (5)	C30–C31	1.392 (5)

(b) Intramolecular Angles (deg)

Cp1–Ir–P	134.1	P–Ir–O	84.37 (6)
Cp1–Ir–O	123.4	P–Ir–H(Ir)	86.0 (11)
Cp1–Ir–H(Ir)	124.9	O–Ir–H(Ir)	90.2 (11)
Ir–O–C11	120.7 (2)	O–C11–C13	113.2 (3)
O–C11–C12	107.6 (3)	C12–C11–C13	111.2 (3)
Ir–P–C14	118.30 (9)	C14–P–C20	104.46 (14)
Ir–P–C20	110.95 (10)	C14–P–C26	98.64 (13)
Ir–P–C26	117.52 (10)	C20–P–C26	105.24 (14)
C2–C1–C5	107.2 (3)	C3–C2–C7	125.8 (3)
C1–C2–C3	107.6 (3)	C2–C3–C8	125.2 (3)
C2–C3–C4	109.4 (3)	C4–C3–C8	125.0 (3)
C3–C4–C5	106.0 (3)	C3–C4–C9	128.2 (3)
C1–C5–C4	109.8 (3)	C5–C4–C9	125.4 (3)
C2–C1–C6	125.9 (3)	C1–C5–C10	127.0 (3)
C5–C1–C6	126.4 (3)	C4–C5–C10	123.2 (3)
C1–C2–C7	125.5 (3)		
P–C14–C15	120.6 (2)	C21–C20–C25	118.2 (3)
P–C14–C19	121.1 (2)	C20–C21–C22	119.9 (3)
P–C20–C21	123.9 (2)	C21–C22–C23	120.7 (3)
P–C20–C25	117.4 (2)	C22–C23–C24	120.1 (3)
P–C26–C27	117.3 (2)	C23–C24–C25	120.0 (3)
P–C26–C31	124.8 (2)	C20–C25–C24	121.0 (3)
C15–C14–C19	118.2 (3)	C27–C26–C31	117.8 (3)
C14–C15–C16	119.9 (3)	C26–C27–C28	121.0 (3)
C15–C16–C17	120.5 (3)	C27–C28–C29	120.2 (4)
C16–C17–C18	119.9 (3)	C28–C29–C30	119.9 (3)
C17–C18–C19	120.2 (3)	C29–C30–C31	120.2 (4)
C14–C19–C18	121.3 (3)	C26–C31–C30	120.9 (3)

[a] Cp1 is the centroid of the cyclopentadiene ring.

data collection parameters are given in Table I and in the Experimental Section. The structure was solved by Patterson methods and refined via standard least-squares and Fourier techniques. An ORTEP drawing and labeling scheme are given in Figure 1; interatomic bond distances and angles are listed in Table II. The geometry around the Ir atom does not suggest any interaction between the oxygen or other atoms and the metal hydride, which was located successfully.

Only a few late-transition-metal alkoxide complexes have been structurally characterized. A recent review[4a] pointed out that many of these (M = Pd, Pt, Ir) feature alkoxide O–C distances that vary between 1.26 and 1.38 Å, which are shorter than those found for free alcohols, especially when O is bound to an sp^3 carbon. The O–C (isopropoxy) distance of 1.407 (3) Å suggests that such short bonds are not necessarily a general feature of late-transition-metal alkoxides (see Table III). The Ir–O distances of 2.076 (2) Å and Ir–O–C angle of 120.7 (2)°, however, are similar to those observed in the 4- and 5-coordinate iridium alkoxides reported previously.

Table III. Crystal Structure Data for Iridium Alkoxides

compd	Ir–O, Å	O–C, Å	∠Ir–O–C, deg
trans-$(PPh_3)_2Ir(CO)(OPh)$[a]	2.049 (4)	1.324 (6)	126.5 (3)
trans-$(PPh_3)_2Ir(CO)(OC_6F_5)$[b]	2.058 (3)	1.302 (6)	135.4 (3)
$(PPh_3)_2Ir(CO)(OPh)(SO_4)$[c]	2.206 (10)	1.385 (21)	118.2 (10)
$(PPh_3)_2Ir(CO)(OPh)(TCNE)$[d]	2.057 (8)	1.232 (15)	137.4 (9)
$[cis\text{-}(PMe_3)_4Ir(OMe)(H)]^+$[e]	2.118 (8)	1.334 (16)	119.4 (9)
$Cp^*IrPPh_3(O\text{-}i\text{-}Pr)(H)$[f]	2.076 (2)	1.407 (3)	120.7 (2)

[a] Rees, W. M.; Churchill, M. R.; Fettinger, J. C.; Atwood, J. D. *Organometallics* **1985**, *4*, 2179. [b] Churchill, M. R.; Fettinger, J. C.; Rees, W. M.; Atwood, J. D. *J. Organomet. Chem.* **1986**, *308*, 361. [c] Severely disordered. Fettinger, J. C.; Churchill, M. R.; Bernard, K. A.; Atwood, J. D. *J. Organomet. Chem.* **1988**, *340*, 377. [d] Janik, T. S.; Bernard, K. A.; Churchill, M. R.; Atwood, J. D. *J. Organomet. Chem.* **1987**, *323*, 247. [e] Milstein, D.; Calabrese, J. C.; Williams, I. D. *J. Am. Chem. Soc.* **1986**, *108*, 6387. [f] This work.

Scheme V

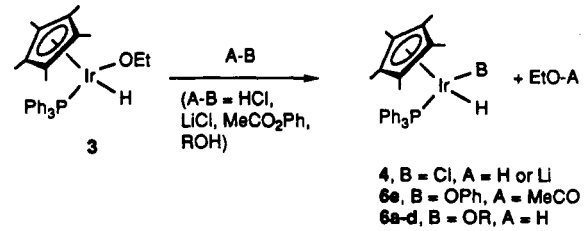

Scheme VI

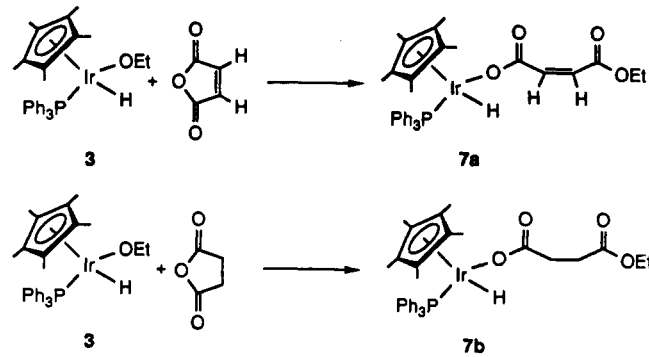

Alkoxide Metatheses. Metatheses similar to those postulated for alcohol exchange occur when ethoxide **3** is treated with HCl or LiCl to give the known $Cp^*IrPPh_3(Cl)(H)$.[11] The ethoxide complex reacts slowly with phenyl acetate to give phenoxy complex **6e** and ethyl acetate (89% by GC). It does not react, however, with methyl acetate. Similar transesterifications have been observed in early-transition-metal systems.[26] We propose (Scheme V) that these reactions, like the alcohol exchange described above, proceed via interaction of the Lewis basic ethoxide oxygen with the Lewis acidic portion of the substrate (RO*H*, H^+, Li^+, PhO*C*(O)Me). Ir–O bond cleavage accompanied by coordination of iridium to the nucleophilic part of the substrate (Cl^-, R*O*H, Ph*O*C(O)Me) may then occur to give the observed products.

Analogous interactions seem to occur in the reaction of **3** with cyclic anhydrides, where the nucleophilic ethoxide participates in an iridium-assisted ring opening (Scheme VI). Thus, reaction of **3** with maleic anhydride gives

(26) Reference 2a, pp 180–183.

Scheme VII

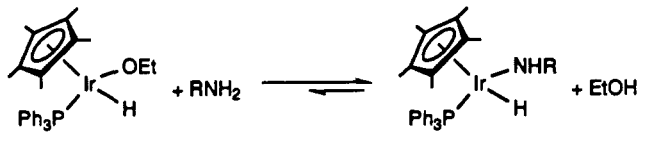

8a, R = Ph
8b, R = CH_2Ph

$Cp^*IrPPh_3[OC(O)CHCHCO_2Et](H)$ (**7a**). In the ^1H NMR spectrum, the alkene protons of **7a** appear as complex multiplets at δ 5.5–5.47 and the ethoxide methylene protons shift downfield to δ 4.12–4.04; in the ^{13}C spectrum the alkene carbons resonate at δ 136.4 and 122.2 (similar to the result for the free alkene: δ 137.5) and the carbonyl carbons are inequivalent. Presumably, this reaction occurs by coordination of the anhydride oxygen to Ir accompanied by attack of ethoxide on the electrophilic carbonyl carbon. The presence of a double bond is not required; succinic anhydride readily undergoes the same reaction. The product in this case, $Cp^*IrPPh_3[OC(O)CH_2CH_2CO_2Et](H)$ (**7b**), is spectroscopically similar to **7a**.

Synthesis of Iridium Amide Hydrides. The alcohol metathesis reaction may be extended to the synthesis of amide complexes. Treatment of **3** with excess aniline or benzylamine affords $Cp^*IrPPh_3(NHR)(H)$ where R = Ph (**8a**) and CH_2Ph (**8b**). This transformation may also be carried out, less conveniently, with an excess of the appropriate lithium amide.[27] The equilibrium nature of the alcohol/amine exchange (Scheme VII) can be demonstrated by ^1H NMR spectroscopy.

The equilibrium constants for these metatheses are directly related to the Ir–O, Ir–N, H–O, and H–N bond dissociation energies (BDE's). If $\Delta G \sim \Delta H$, ΔG = BDE(H–OEt) + BDE(Ir–NHR) – [BDE(Ir–OEt) + BDE(H–NHR)]. In the case of R = Ph in Scheme VII, BDE(N–H) in aniline is ~88 kcal/mol, BDE(O–H) in ethanol is ~104 kcal/mol,[28] and the equilibrium lies to the right, but not strongly so ($K_{eq} \sim 10$). This suggests that the Ir–OEt bond is appreciably stronger than the Ir–NHPh bond in this system; if the opposite were true the equilibrium concentration of ethoxy hydride would not be detectable. Qualitatively, the equilibrium with benzylamine ($K_{eq} \sim 1$) lies less far to the right than does that with aniline, consistent with the weaker N–H bond in the latter case. Quantitative comparison of the Ir–NHPh and Ir–$NHCH_2Ph$ bond strengths is impossible without more accurate values for the equilibrium constants and the benzylamine N–H BDE.

The amido hydride compounds **8a,b** are spectroscopically similar to the alkoxides. The Cp^*IrPPh_3H portion is readily identified by ^1H, ^{13}C, and ^{31}P NMR spectroscopy. In the anilide complex **8a**, the NH proton appears at δ 1.24 (THF-d_8) and coupling to phosphorus (J = 4.2 Hz) is observed. When this complex is prepared from **3** and $PhND_2$ to give $Cp^*IrPPh_3(NDPh)(H)$ (**8a**-*N*-d_1), this peak does not appear but the metal hydride is unchanged. The NH stretch in the infrared spectrum at 3357 cm^{-1} shifts on deuteration to 2492 cm^{-1}; ν_{NH}/ν_{ND} = 1.35. Preparation of ^{15}N-labeled **8a**-^{15}N from labeled aniline gives rise to a doublet of doublets due to the N–H proton, with J_{NH} = 75 Hz and J_{PH} = 4.5 Hz. Reaction of $Cp^*IrPPh_3(OCD_2CD_3)(D)$ (**3**-d_6) with aniline gives Cp^*IrPPh_3(NHPh)(D) (**8a**-*Ir*-d_1) with ν_{IrD} = 1530 cm^{-1} (ν_{IrH}/ν_{IrD} = 1.39). In the carbon NMR spectrum, the N-bound phenyl ring in **8a** gives rise to four signals (ipso, meta, ortho, and para) but in benzylamido complex **8b** six different phenyl carbons are observed. Similar restricted rotation of an Ir-bound amide was reported[29] for $[(Cp^*Ir)_2(\mu\text{-}OH)_2(\mu\text{-}NHPh)]^+$. Anilide complex **8a** is thermally stable, but the benzylamide **8b** slowly decomposes in solution at room temperature, in accord with the generally greater kinetic stability of anilides vis-à-vis amides.[2b,4b]

Scheme VIII

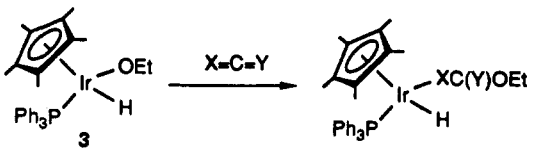

9, X=Y=O
10, X=Y=S
11a, Y=O, X = NPh
11b, Y=O, X = Np-Tol
11c, Y=O, X = NMe

Like the alkoxy hydrides discussed above, amido hydride species are rare, although several compounds with chelating hybrid P–N ligands[30] are known. Recently, iridium amide hydrides[31] have been prepared and crystallographically characterized, and Cowan and Trogler reported the synthesis, structure and reactivity of *trans*-$Pt(PEt_3)_2$(NHPh)(H).[32]

Insertion Reactions of Iridium Alkoxide and Amide Hydrides. Heterocumulenes CO_2, CS_2, and RNCO are known to insert into the M–O bond of metal alkoxides to form new compounds with metal–S, –N, and –O bonds.[33] These small molecules have also been reported to undergo formal insertion into M–H bonds; for example, carbon dioxide reacts with $[HW(CO)_5]^-$ to give a metal formate.[34] The reaction of ethoxy hydride complex **3** with CO_2 and its analogues provides an interesting example of M–O vs M–H selectivity; we observe only insertion into the Ir–O bond, as shown in Scheme VIII.

The reaction of **3** with carbon dioxide affords $Cp^*IrPPh_3(OCO_2Et)(H)$ (**9**) as the major component of a mixture. This metallocarbonate compound was identified by its IR spectrum (ν_{IrH} = 2040 cm^{-1}, ν_{OCO} = 1662, 1280 cm^{-1}) and its ^1H NMR spectrum (signals due to ethoxide and hydride). Complex **9** decomposes at room temperature and could not be isolated.

The product of carbon disulfide insertion, $Cp^*IrPPh_3(S_2COEt)(H)$ (**10**), however, was thermally stable and could be isolated in good yield. The iridium hydride is observed at δ –13.79 (d, J_{HP} = 34.3) in the ^1H NMR spectrum and at 2085 cm^{-1} in the IR spectrum, which also contains xanthate stretches at 1265, 1110, and 1050 cm^{-1}.[35] The sulfur-bound carbon appears at δ 224.1 in the ^{13}C NMR spectrum; the lack of ^{13}C–^{31}P coupling for this signal is

(27) We thank Dr. Jeffrey Stryker for preliminary studies of this reaction in these laboratories.
(28) Values from: McMillen, D. F.; Golden, D. M. *Annu. Rev. Phys. Chem.* **1982**, *33*, 493.
(29) Nutton, A.; Maitlis, P. M. *J. Chem. Soc., Dalton Trans.* **1981**, 2339.
(30) (a) Reference 4b and references therein. (b) Park, S.; Johnson, M. P.; Roundhill, D. M. *Organometallics* **1989**, *8*, 1700 and references therein.
(31) (a) Casalnuovo, A. L.; Calabrese, J. C.; Milstein, D. *Inorg. Chem.* **1987**, *26*, 973. (b) Casalnuovo, A. L.; Calabrese, J. C. *J. Am. Chem. Soc.* **1988**, *110*, 6738.
(32) (a) Cowan, R. L.; Trogler, W. C. *Organometallics* **1987**, *6*, 2451. (b) Cowan, R. L.; Trogler, W. C. *J. Am. Chem. Soc.* **1989**, *111*, 4730.
(33) Reference 2a, pp 281–298.
(34) Darensbourg, D. J.; Ovalles, C. *J. Am. Chem. Soc.* **1984**, *106*, 3750.
(35) Nakamoto, K. *Infrared and Raman Spectra of Inorganic and Coordination Compounds*; Wiley-Interscience: New York, 1986; pp 342–249.

Scheme IX

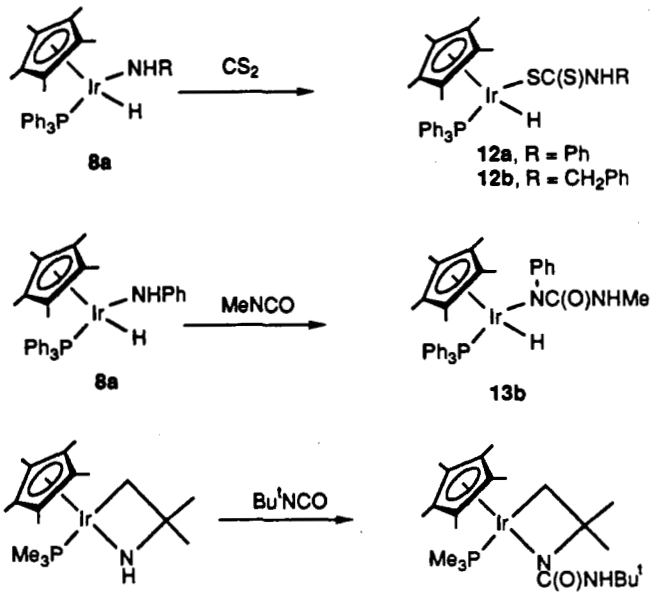

consistent with the proposed atom connectivity and rules out the isomer Ir–C(S)S–OEt.

Aryl and alkyl isocyanates react with **3** to give $Cp^*IrPPh_3(NRCO_2Et)(H)$ (**11a–c**) (R = Ph, *p*-Tol, Me). The aryl complexes were isolated in high yield but the reaction with methyl isocyanate gives small amounts of other hydride-containing products which could not be separated from the insertion product. These compounds have ^1H NMR, ^{13}C NMR, and IR spectra characteristic of the Cp^*IrPPh_3H fragment, including hydride absorptions at δ −14.95 (d, J_{HP} = 38.0) and 2136 cm^{-1} for the phenyl derivative. This compound also features an IR absorption at 1643 cm^{-1} and a signal at δ 158.8 in the ^{13}C NMR spectrum due to the carbonyl group.

Similar insertion chemistry is observed with the amido hydride compounds (Scheme IX). Anilide complex **8a** reacts with carbon disulfide to form $Cp^*IrPPh_3(SC(S)NHPh)(H)$ (**12a**), which exhibits a characteristic N–H signal in the ^1H NMR at δ 11.20. The intensity of this peak decreases dramatically when the deuterium-labeled precursor Ir–NDPh is used. Insertion of carbon disulfide into the N–H bond, as observed for organic amines, was discounted by an ^{15}N labeling study; the N–H proton in the labeled compound gives rise to a doublet centered at δ 11.20 with a ^{15}N–H coupling of 87 Hz. The thiocarbamic acid derivative formed by the insertion of CS_2 into the N–H bond would not be expected to exhibit this coupling. The CS_2 carbon resonates at δ 201.0 in the carbon spectrum. The FAB mass spectrum showed the expected molecular ion at *m/e* 759/757. Unfortunately, satisfactory elemental analysis could not be obtained and the aromatic region of the carbon NMR spectrum contained more signals than expected for this compound. The benzylamide derivative $Cp^*IrPPh_3(SC(S)NHCH_2Ph)(H)$ (**12b**) was more tractable; in this case the carbon spectrum was unexceptional and the material analyzed correctly for C, H, and N, while displaying spectroscopic features similar to those observed for the anilide derivative, including a signal assigned to N–H in the ^1H NMR spectrum at δ 9.23.

Reaction of anilide **8a** with methyl isocyanate, however, gives $Cp^*IrPPh_3(NPhC(O)NHMe)(H)$ (**13b**), the product of nucleophilic attack of the anilide on the isocyanate carbonyl, equivalent to insertion of isocyanate into the N–H bond. Such reactions are observed in the metal-free reaction of amines and isocyanates, and recently in an iridium amide complex in our laboratories.[36] The metallacycle $Cp^*IrPMe_3(CH_2CMe_2NH)$ reacted with *tert*-butyl isocyanate to give $Cp^*IrPMe_3(CH_2CMe_2N(C(O)NH\text{-}t\text{-}Bu)$ (**13a**), which is spectroscopically similar to **13b**.

Metallacycle **13a** displays ν_{CO} = 1601 cm^{-1} and δ 159.5 for the isocyanate carbonyl carbon. For compound **13b**, ν_{CO} appears at 1615 cm^{-1} (another strong band at 1581 cm^{-1} is probably due to a C–C phenyl stretch, a type of absorption that is often observed in this region for this series of compounds) and the carbonyl carbon resonates at δ 162.6. When this compound is prepared from its ^{15}N-labeled precursor, ^{15}N–^{13}C coupling is observed both for this carbon (J = 15.5 Hz) and for the ipso NC_6H_5 carbon (J = 10 Hz).

Scheme X

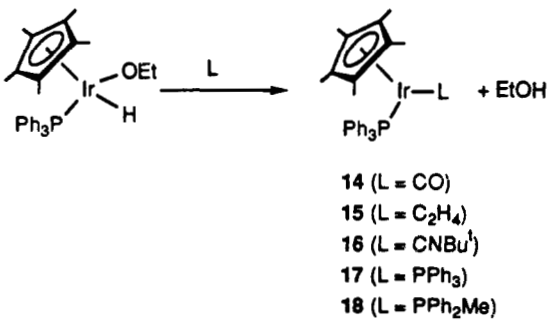

Elimination Reactions of Iridium Alkoxide and Amide Hydrides. Insertions of carbon monoxide, isocyanide, and alkenes into metal–oxygen bonds have been reported,[37] but the reaction of ethoxy hydride complex **3** with these substrates takes a different course (Scheme X). In all cases ethanol is eliminated in quantitative yield (^1H NMR spectroscopy and GC) and the corresponding Ir(I) complex Cp^*IrPPh_3L (L = CO, C_2H_4, CN-*t*-Bu) (**14–16**) is formed. These reactions do not proceed by simple reductive elimination of ethanol followed by trapping of the 16-electron Cp^*IrPPh_3 species by ligand, as demonstrated by kinetic studies (see below). Such a pathway should also lead to the orthometalated complex $Cp^*Ir(PPh_2C_6H_4)(H)$ (**5a**), which is not observed. This ligand-induced reductive elimination also proceeds with the phosphines PPh_3 and PPh_2Me to form $Cp^*Ir(PPh_3)_2$ (**17**) and $Cp^*Ir(PPh_3)(PPh_2Me)$ (**18**).

The triphenylphosphine carbonyl complex **14** was characterized by IR (ν_{CO} = 1923 cm^{-1}) and ^{13}C NMR (δ 181.3, d, J_{PC} = 15.1 Hz for IrCO) spectroscopy. Ethylene complex **15** displayed signals due to coordinated ethylene protons at δ 1.1 in the ^1H NMR spectrum. The ethylene carbons appear at δ 14.6 in the carbon spectrum. The *tert*-butyl isocyanide compound **16** was characterized by its IR spectrum (ν_{CN} = 1872 cm^{-1}) and its ^{13}C NMR signal at δ 179.9 (d, J_{PC} = 16.6 Hz) due to the iridium-bound isonitrile carbon. Bis(triphenylphosphine) complex **17** gave rise to a singlet in the phosphorus NMR spectrum at δ 20.7, and three of the four triphenylphosphine carbons appear as virtual triplets in the ^{13}C spectrum due to coupling to the two phosphorus atoms. The mixed bis(phosphine) complex **18** displayed the expected AX pattern in the phosphorus NMR spectrum with a P–P coupling of 25.9 Hz.

(36) Klein, D. P.; Hayes, J. C.; Bergman, R. G. *J. Am. Chem. Soc.* **1988**, *110*, 3704.

(37) For examples of CO and alkene insertion see: Bryndza, H. *Organometallics* **1985**, *4*, 406 and references therein. For a recent example of isocyanide insertion see: Erikson, T. K. G.; Bryan, J. C.; Mayer, J. M. *Organometallics* **1988**, *7*, 1930.

Scheme XI

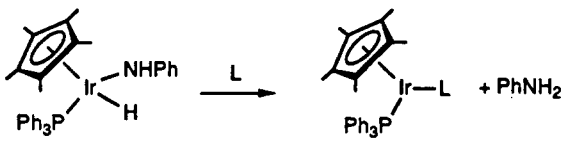

8a

14 (L = CO)
15 (L = C_2H_4)
16 (L = $CNBu^t$)
17 (L = PPh_3)
18 (L = PPh_2Me)

Scheme XII

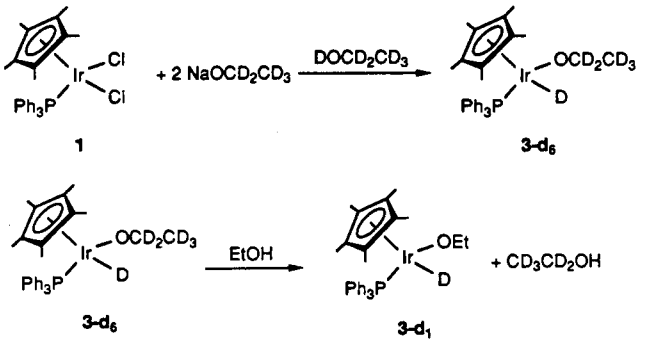

The anilido hydride complex $Cp^*IrPPh_3(NHPh)(H)$ (**8a**) undergoes similar reactions with PPh_3, PPh_2Me, CO, C_2H_4, and CN-*t*-Bu, forming aniline (GC) and the appropriate Ir–L compounds (Scheme XI). Similarly, benzylamide complex **8b** reacts with PPh_3 to form benzylamine and $Cp^*Ir(PPh_3)_2$.

Kinetic Studies of Ligand-Induced Reductive Elimination. Unlike reductive eliminations featuring C–H and C–C bond formation,[38] eliminations resulting in N–H and O–H bond formation have not been extensively studied, so an understanding of their mechanisms is of interest. In contrast to C–H reductive elimination in the closely related system $Cp^*IrPMe_3(Cy)(H)$ (Cy = *c*-C_6H_{11}),[12] the O–H and N–H eliminations reported here proceed at ambient temperature and do not occur without added phosphine, while cyclohexane formation occurs at 130 °C at a rate that is unaffected by added phosphine.

Thermally induced reductive elimination from $Cp^*Ir(PMe_3)(Cy)(H)$ gave cyclohexane formed from the cyclohexyl and hydride groups; $Cp^*Ir(PMe_3)(Cy)(D)$ yielded cyclohexane-d_1.[12] The ethanol produced on treatment of **3** with PPh_3 appears to be formed similarly from combination of the ethoxide and hydride ligands. However, isobutane formed from $Cp^*_2Zr(i\text{-}Bu)(H)$ is generated from the isobutyl group and a Cp* methyl hydrogen.[39] Our recent observation[40a] that the related anilide compound $Cp^*IrPPh_3(Me)(NHPh)$ reacts with 1,2-bis(diphenylphosphino)ethane (dppe) to give aniline and the product of deprotonation of a Cp* methyl group, $(\eta^4\text{-}C_5Me_4CH_2)Ir(dppe)Me$, raised the possibility that hydrogen from a Cp* methyl could appear in the observed ethanol.

To test this possibility, the ethoxy deuteride complex $Cp^*IrPPh_3(OEt)(D)$ (**3**-d_1) was prepared (Scheme XII). Reaction of $Cp^*IrPPh_3Cl_2$ with $NaOCD_2CD_3$ in CD_3CD_2OD gave $Cp^*IrPPh_3(OCD_2CD_3)(D)$ (**3**-d_6).[41] Exchange of ethanol for OCD_2CD_3 in **3**-d_6 gave **3**-d_1. Analysis of the ethanol formed on reaction of **3**-d_1 with PPh_3 was hampered by loss of some deuterium, perhaps by exchange of the hydroxyl protons on the surface of the glassware. Direct observation by ^2H NMR spectroscopy of this reaction in C_6H_6 showed the formation of EtOD in 64% yield and no incorporation of deuterium into the Cp* methyl groups. On a large scale, EtOD(H) was trapped with $LiCPh_3$ and the resulting $Ph_3CD(H)$ analyzed by ^1H and ^2H NMR spectroscopy, which demonstrated ~40% D incorporation. These results suggest that the ethanol is produced (like cyclohexane in the C–H case) by O–H elimination from the metal center. Further experiments bearing on this point are described below.

Table IV. Rate Data for Reactions of (a) $Cp^*IrPPh_3(OEt)(H)$ (3) with PPh_3 in Toluene at 10 °C, (b) $Cp^*IrPPh_3(OEt)(D)$ with PPh_3 in Toluene at 10 °C, and (c) $Cp^*IrPPh_3(OEt)(H)$ with PPh_3 in DMF at 10 °C

a		b		c	
$[PPh_3]$, M	10^4k_{obs}, s^{-1}	$10^2[PPh_3]$, M	10^4k_{obs}, s^{-1}	$[PPh_3]$, M	10^4k_{obs}, s^{-1}
7.80×10^{-2}	3.42	7.46	4.16	3.24×10^{-2}	5.76
5.85×10^{-2}	3.51	6.63	4.13	2.16×10^{-2}	4.93
2.59×10^{-2}	3.49	5.97	4.24	1.08×10^{-2}	4.77
1.30×10^{-2}	3.04	4.98	4.32	8.64×10^{-3}	4.61
9.07×10^{-3}	2.76	3.32	4.28	7.20×10^{-3}	4.01
6.48×10^{-3}	2.45			4.32×10^{-3}	2.49
5.44×10^{-3}	1.97			2.70×10^{-3}	2.24
4.35×10^{-3}	1.85			2.33×10^{-3}	1.88
3.89×10^{-3}	2.05			2.16×10^{-3}	1.45
2.59×10^{-3}	1.66				

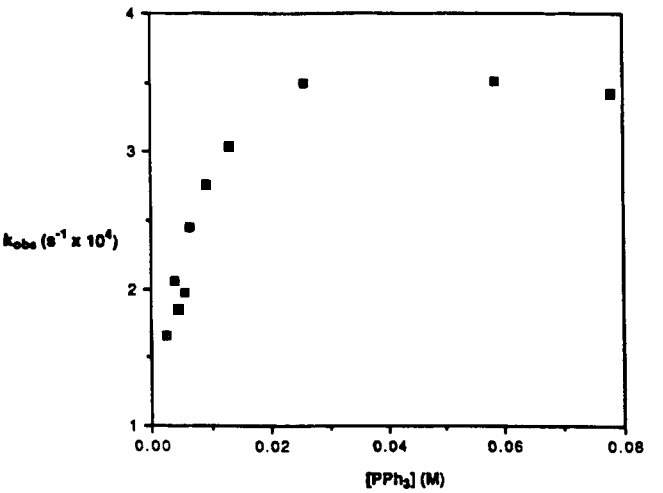

Figure 2. Plot of k_{obs} vs $[PPh_3]$ for the reaction of $Cp^*IrPPh_3(OEt)(H)$ (**3**) with PPh_3 in toluene at 10 °C.

The rate of the reaction of $Cp^*IrPPh_3(OEt)(H)$ and PPh_3 to give ethanol and $Cp^*Ir(PPh_3)_2$ was measured in toluene at 10 °C by UV–visible spectroscopy. The appearance of product was monitored by its absorbance at 355 nm over at least 3 half-lives. Runs were performed over the phosphine concentration range 2.59×10^{-3} to 7.80×10^{-2} M. Plots of absorbance vs time were fit to an increasing exponential function from which values for the infinity point and the rate constant could be extracted. Table IV shows the observed rates.

(38) Reference 1, pp 279–355.
(39) McAlister, D. R.; Erwin, D. K.; Bercaw, J. E. *J. Am. Chem. Soc.* **1978**, *100*, 5966.
(40) (a) Glueck, D. S.; Bergman, R. D. *Organometallics* **1990**, *9*, 2862. (b) Glueck, D. S.; Bergman, R. D. *Organometallics*, following paper in this issue.
(41) Under these conditions, some incorporation of deuterium into the Cp* ligand (~5–10% by ^1H and ^2H NMR analysis) occurred. This phenomenon is also observed when the dichloride is treated with $NaOCH_2CH_3$ in CH_3CH_2OD or with $NaOCD_2CH_3$ in CH_3CD_2OH. Presumably, this occurs by deprotonation/protonation of Cp* methyl groups. Such deuterium incorporation has been observed previously in related Cp*Rh compounds: Nutton, A.; Maitlis, P. M. *J. Chem. Soc., Dalton Trans.* **1981**, 2335 and ref 3 therein.

A plot of triphenylphosphine concentration vs the rate of product formation gave typical saturation kinetics (Figure 2). These data are consistent with the reversible formation of an intermediate X that can be trapped by phosphine.

$$Cp^*IrPPh_3(OEt)(H) \underset{k_{-1}}{\overset{k_1}{\rightleftharpoons}} X \xrightarrow[-EtOH]{k_2[PPh_3]} Cp^*Ir(PPh_3)_2 \quad (1)$$

With the steady-state approximation that the instantaneous concentration of X is zero, the rate law

$$k_{obs} = k_1k_2[L]/(k_{-1} + k_2[L]) \quad (2)$$

where L = PPh_3, is obtained. For low [L]

$$k_{-1} \gg k_2[L] \quad \text{and} \quad k_{obs} = k_1k_2[L]/k_{-1} \quad (3)$$

In this regime, k_{obs} increases with [L], giving rise to the increasing portion of the saturation plot. For large [L]

$$k_{-1} \ll k_2[L] \quad \text{and} \quad k_{obs} = k_1 \quad (4)$$

In this case, intermediate X is trapped by PPh_3 essentially every time it is formed, and further increases in [L] have no effect on the rate, giving the constant-rate "saturation" portion of the graph.

The inverse expression

$$1/k_{obs} = k_{-1}/k_1k_2[L] + 1/k_1 \quad (5)$$

can be used to extract the quantities of k_1 and k_{-1}/k_2 from a plot of $1/k_{obs}$ vs $1/[L]$.

The rate measurements that we have made on the reaction of $Cp^*IrPPh_3(OEt)(H)$ with PPh_3 deserve some comment, because we encountered some frustrating difficulties in reproducibility. Our measurements were repeated at different times and by different individuals. We always observed saturation behavior, and the rates were qualitatively similar in all cases; we therefore believe that the k_1 and k_{-1}/k_2 values, and the conclusions drawn from them, are qualitatively correct. However, although individual runs showed good reproducibility, measurements made months or years apart gave somewhat different results. We do not know if these variations are due to impurities in the samples or to small temperature fluctuations. However, because of this problem, it is difficult to know exactly what our realistic error limits are. A plot of $1/k_{obs}$ vs $1/[L]$ gave a reasonably straight line ($R^2 = 0.92$). On the basis of the analysis summarized above the slope of this plot should be k_{-1}/k_1k_2 and the y intercept $1/k_1$, so from the data $k_1 = 3.7 \times 10^{-4}$ s^{-1} and $k_{-1}/k_2 = 3.4 \times 10^{-3}$ M. In view of the uncertainties mentioned above, however, and the fact that the data in Table VI (which will be discussed below) also show variation in the measured value for k_1, we estimate that the most reliable value for this rate constant is 4 ($\pm$1) $\times 10^{-4}$ s^{-1}, and values quoted for the other rate constants may well have error limits of similar magnitude.

The rate of PPh_3-induced ethanol formation from **3**-d_1 was measured under conditions identical with those used for **3** at high PPh_3 concentrations to ensure saturation. The observed rates are given in Table IVb; the average value of k_1 is 4.2×10^{-4} s^{-1}. Within experimental error, this rate is the same as that observed for unlabeled **3**. The large errors associated with the measured rates make this experiment inconclusive; a kinetic isotope effect smaller than 1.5 probably could not confidently be ruled out.

The rate of the same O–H elimination was measured, again at 10 °C, in the polar aprotic solvent dimethylformamide (DMF) for comparison to toluene. The data are shown in Table IVc. The solvent effect is small; the rate-determining k_1 step proceeds about twice as fast in DMF as in toluene: $k_1 = 8.0 \times 10^{-4}$ s^{-1} and $k_{-1}/k_2 = 8.4 \times 10^{-3}$ M ($R^2 = 0.94$).

Table V. Rate Data for Reaction of $Cp^*Ir[P(p\text{-}XC_6H_4)_3](OEt)(H)$ (X = Me (20b), MeO (20c), F (20a)) with PPh_3 in Toluene at 10 °C

20b		20c		20a	
[PPh_3], M	10^4k_{obs}, s^{-1}	[PPh_3], M	10^4k_{obs}, s^{-1}	[PPh_3], M	10^4k_{obs}, s^{-1}
3.90×10^{-2}	3.05	2.59×10^{-2}	2.56	2.89×10^{-2}	3.20
2.59×10^{-2}	3.15	1.94×10^{-2}	2.56	2.17×10^{-2}	3.29
1.94×10^{-2}	3.11	1.29×10^{-2}	2.42	1.45×10^{-2}	3.24
1.30×10^{-2}	2.88	1.04×10^{-2}	2.35	1.16×10^{-2}	3.15
9.06×10^{-3}	2.72	7.77×10^{-3}	2.28	8.68×10^{-3}	2.95
7.77×10^{-3}	2.70	5.18×10^{-3}	1.94	7.23×10^{-3}	3.03
6.48×10^{-3}	2.56	3.89×10^{-3}	1.68	5.79×10^{-3}	3.00
5.18×10^{-3}	2.40	2.89×10^{-3}	1.77	4.34×10^{-3}	2.79
3.88×10^{-3}	2.11	2.59×10^{-3}	1.53	1.45×10^{-3}	2.12
2.59×10^{-3}	1.77				

Table VI

(a) Rate Data for Reaction of $Cp^*IrPPh_3(OEt)(H)$ (**3**) with $P(p\text{-}XC_6H_4)_3$ (X = Me (a), F (b)) in Toluene at 10 °C

a		b	
[PAr_3], M	10^4k_{obs}, s^{-1}	[PAr_3], M	10^4k_{obs}, s^{-1}
2.36×10^{-2}	3.81	3.14×10^{-2}	4.67
1.77×10^{-2}	3.60	1.57×10^{-2}	4.69
1.06×10^{-2}	3.11	1.26×10^{-2}	4.57
9.44×10^{-3}	3.07	1.10×10^{-2}	4.44
8.26×10^{-3}	2.84	9.43×10^{-3}	4.41
7.06×10^{-3}	2.58	7.86×10^{-3}	4.20
5.90×10^{-3}	2.45	6.29×10^{-3}	4.03
4.72×10^{-3}	2.21	4.72×10^{-3}	3.75
3.54×10^{-3}	1.86	3.14×10^{-3}	3.32
2.36×10^{-3}	1.48		

(b) Kinetics of the Reaction $Cp^*IrPPh_3(OEt)(H) + P(p\text{-}XC_6H_4)_3$ in Toluene

X	10^4k_1, s^{-1}	$10^3k_{-1}/k_2$, M	k_2(rel)[a]	k_2(rel)[b]
H	3.7	3.4	1.0	1.0
Me	4.6	5.0	1.5	1.6
F	5.1	1.7	0.49	0.53
MeO				1.4

[a] k_2(rel) = k_2 for PPh_3/k_2 for PAr_3. These values were determined at 10 °C. R^2 values: 1.0 for X = Me; 0.99 for X = F. [b] Determined in direct competition studies by ^1H and $^{31}P\{^1H\}$ NMR spectroscopy at room temperature.

The Ir-bound triphenylphosphine ligand was systematically varied in hopes of observing an electronic effect on the rate of ethanol formation. The required triarylphosphine-substituted ethoxy hydride complexes $Cp^*IrP(p\text{-}XC_6H_4)_3(OEt)(H)$ (**20a–c**, X = F, Me, MeO) were prepared straightforwardly by the same route as for the PPh_3 compound, and the mixed bis(phosphine) products $Cp^*Ir(PPh_3)(PAr_3)$ (**21a–c**) by addition of the appropriate phosphine to the parent ethoxide compound. The observed rates are given in Table V. From these data, the rate constants are as follows: X = Me $k_1 = 3.4 \times 10^{-4}$ s^{-1}, $k_{-1}/k_2 = 2.4 \times 10^{-3}$ M, $R^2 = 0.99$; X = F $k_1 = 3.4 \times 10^{-4}$ s^{-1}, $k_{-1}/k_2 = 8.5 \times 10^{-4}$ M, $R^2 = 0.98$; X = MeO $k_1 = 2.8 \times 10^{-4}$ s^{-1}; $k_{-1}/k_2 = 2.0 \times 10^{-3}$ M, $R^2 = 0.93$. Only small rate changes were observed, and within the limits of measurement the substitutions had no effect on k_1, the rate of formation of intermediate X.

Similarly, further information on the nature of X can be obtained by measuring the partitioning of this intermediate between starting material and product. The rate of reaction of $Cp^*IrPPh_3(OEt)(H)$ with the para-substituted phosphines described above to form EtOH and the mixed phosphine complexes $Cp^*Ir(PPh_3)(PAr_3)$ was measured in toluene at 10 °C. The observed rates and the derived rate constants are given in Table VIa,b. Since k_{-1} must be the same in each case, relative k_2 (trapping) rate constants can be obtained for each phosphine. The

Table VII. Rate Data for Reaction of $Cp^*IrPPh_3(NHR)(H)$ (8a,b) with PPh_3 in Toluene at 10 °C (R = CH_2Ph (8b)) and at 45 °C (R = Ph (8a))

8b		8a	
$[PPh_3]$, M	10^4k_{obs}, s^{-1}	$[PPh_3]$, M	10^4k_{obs}, s^{-1}
2.82×10^{-2}	3.07	2.82×10^{-2}	2.39
1.41×10^{-2}	3.25	1.41×10^{-2}	2.30
5.64×10^{-3}	3.32	7.05×10^{-3}	2.12
4.23×10^{-3}	3.19	5.64×10^{-3}	1.91
2.82×10^{-3}	2.67	4.83×10^{-3}	2.11
1.41×10^{-3}	2.79	4.23×10^{-3}	1.80
1.17×10^{-3}	2.53	2.82×10^{-3}	1.84
7.83×10^{-4}	2.19	1.88×10^{-3}	1.60
5.22×10^{-4}	1.81	1.41×10^{-3}	1.54

Table VIII. Rate Constants for O–H and N–H Reductive Elimination in Toluene $Cp^*IrPPh_3(H)(X) + PPh_3 \rightarrow Cp^*Ir(PPh_3)_2 + HX$

X	10^4k_1, s^{-1}	k_{-1}/k_2, M	t, °C
OEt	3.7	3.4×10^{-3}	10
$NHCH_2Ph$[a]	3.4	4.3×10^{-4}	10
NHPh[a]	2.4	8.6×10^{-4}	45

[a] Correlation coefficients: $NHCH_2Ph$, $R^2 = 0.94$; NHPh, $R^2 = 0.90$.

data in Table VI demonstrate again the error inherent in the measurement of k_1 for ethanol elimination from $Cp^*IrPPh_3(OEt)(H)$ (3).

The trapping ratios were also obtained directly by competition experiments. Treating ethoxy hydride complex 3 with equally high (greater than 10-fold excess) concentrations of two triarylphosphines P_1 and P_2 at ambient temperature leads to the formation of ethanol and the two mixed phosphine complexes $Cp^*Ir(PPh_3)(P_1)$ and $Cp^*Ir(PPh_3)(P_2)$. Phosphine exchange in the products is slow under these conditions, and analysis of the product ratios by NMR spectroscopy gives results consistent with the relative rate constants determined in the direct rate measurements, as shown in Table VIb. According to the data, intermediate X is preferentially trapped by $P(p\text{-}XC_6H_4)_3$ in the order X = F > H > MeO > Me, but once again, the depencence of rate on structure is very small.

A similar study of the triphenylphosphine-induced elimination of amine from the amido hydrides $Cp^*IrPPh_3(NHR)(H)$ (R = Ph, CH_2Ph) in toluene again gave saturation kinetics and rate laws identical with those observed for the ethoxide compound 3. The observed rates are given in Table VII and the rate constants in Table VIII. The reductive elimination of benzylamine proceeds at a rate similar to that for ethanol at 10 °C in toluene, but loss of aniline occurs slowly under these conditions, and a rate of the same magnitude is reached only at 45 °C. This increased kinetic stability of the anilide is echoed for the phenoxide $Cp^*IrPPh_3(OPh)(H)$, which reacts with PPh_3 to form phenol and $Cp^*Ir(PPh_3)_2$ only at 85 °C. At this temperature, however, the phenoxy hydride complex undergoes a side reaction, independent of phosphine, resulting in new unidentified iridium hydride products.

Mechanism of Ligand-Induced Reductive Elimination. As the rate laws for O–H and N–H reductive elimination are the same, it is likely that these reactions proceed via an intermediate of similar structure. Since ethoxy hydride 3 is an 18-electron complex, the intermediate presumably contains an open coordination site to which phosphine can bind, inducing elimination of ethanol. Several plausible alternative structures for this intermediate are illustrated in Scheme XIII.

Concerted reductive elimination of ethanol would give A, the 16-electron Cp^*IrPPh_3, or a solvated analogue. Trapping of this coordinatively unsaturated species with

Scheme XIII

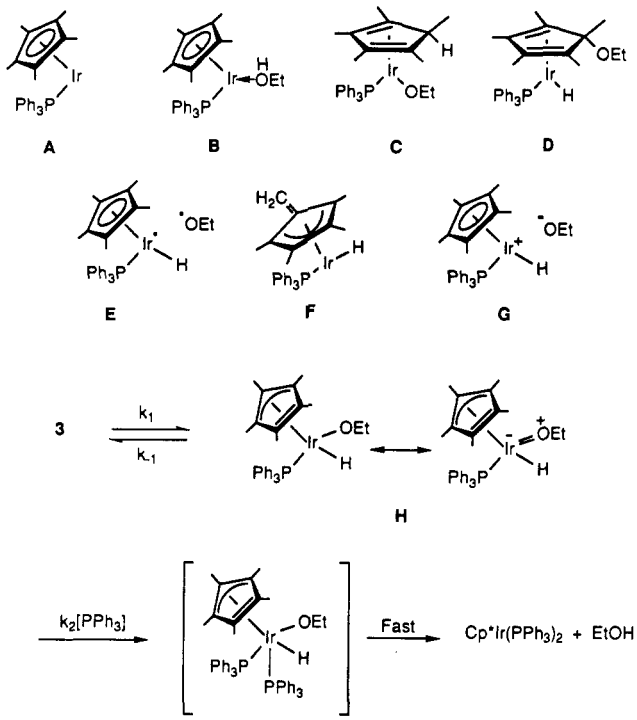

PPh_3 would give the observed products. As discussed above, however, A is thought to be formed on photolytic extrusion of H_2 from $Cp^*IrPPh_3H_2$ or thermal loss of RH from $Cp^*IrPPh_3(R)(H)$. Under these conditions, A oxidatively adds the C–H bonds of its triphenylphosphine ligand in competition with those of the solvent, such as benzene. As these products are not observed in the phosphine-induced ethanol elimination, we conclude that A is not the intermediate X in this process.

Concerted reductive elimination of ethanol to give an ethanol complex would give structure B. Displacement of coordinated ethanol by phosphine in the k_2 step gives the bis(phosphine) product; the coordinatively saturated nature of the intermediate would explain the lack of C–H activation products. Intermediate B, if it exists, must not undergo exchange with free ethanol, since reaction with EtOD would be expected to wash out the metal hydride and replace it with deuterium. As the compounds $Cp^*Ir(PPh_3)L$ usually undergo ligand substitution only at high temperature, this seems plausible, even though ethanol should not be a very good ligand in complex B.

Formation of this intermediate (or of A) would involve Ir–H bond breaking and O–H bond formation in the k_1 step, and the rate of this process should be perturbed by the substitution of Ir–D for Ir–H. Our study of C–H reductive elimination in the alkyl hydride complex $Cp^*IrPMe_3(Cy)(D)$[12] showed an apparent inverse isotope effect and the completely labeled $Cp^*IrPMe_3(Cy\text{-}d_{11})(D)$ undergoes thermal elimination of cyclohexane-d_{12} with $k_H/k_D = 0.7$ (1). This reaction was proposed to go via a cyclohexane σ-complex which should be a good model for ethanol complex B. Unfortunately, the rate data for elimination from 3 and 3-d_1 do not permit a confident assessment of the kinetic isotope effect, so we cannot rule out intermediate B in this way.

However, other experimental evidence suggests that the formation of a σ-complex is unlikely. Thus, if the anilido hydride $Cp^*IrPPh_3(NHPh)(H)$ (8a) undergoes rapid equilibration with the aniline compound $Cp^*IrPPh_3(NH_2Ph)$, scrambling of the deuterium in the labeled analogue $Cp^*IrPPh_3(NDPh)(H)$ (8a-N-d_1) to form

$Cp^*IrPPh_3(NHPh)(D)$ (**8a**-*Ir*-d_1) and in **8a**-*Ir*-d_1 to form **8a**-*N*-d_1 would be expected. Neither of these labeled compounds undergo scrambling at 45 °C in benzene, the conditions required for PPh_3-induced aniline formation. It seems unlikely that reversible N–H bond formation in **8a** could occur with "memory" of the D location.

Intermediate C would be formed by migration of Ir–H to the Cp* ring. This "parking" of a metal hydride on the Cp* ring was proposed for elimination of isobutane from $Cp^*_2Zr(i\text{-}Bu)(H)$.[39] The driving force for this rearrangement is presumably the relief of steric strain. The Ir–H bond strength probably does not change much in the series $Cp^*IrPPh_3(H)(X)$ (X = OEt, OPh, $NHCH_2Ph$, NHPh), so this argument does not rationalize well the experimental result that the more crowded anilide and phenoxide compounds exhibit much lower k_1 values than their alkoxide and amide counterparts.

Similarly, migration of metal-bound ethoxide to the ring would afford complex D. Benfield and Green observed reversible tungsten-to-Cp ethyl group transfer in the reaction of $Cp_2Mo(Et)(Cl)$ with PR_3 to give $[Cp(\eta^4\text{-}C_5H_5Et)MoPR_3(Cl)]$, which gave $[Cp_2Mo(Et)PR_3]^+BF^{4-}$ on treatment with $TlBF_4$.[42] We discount the possibility of this process on steric grounds. Cp* is much more crowded than Cp, and only the small hydride ligand has been proposed to migrate to Cp*. The similar k_1 values observed for ethoxide and benzylamide ligands, despite their differing sizes, suggest that the k_1 step does not involve this sterically demanding transformation.

The radical pair E could be formed by homolytic cleavage of the Ir–O bond. Addition of phosphine to the Ir-centered radical would give a 19-electron species which could undergo hydrogen atom abstraction by ethoxide radical to give the products. Compound **3** does not react with the radical trap dihydroanthracene, and attempts to intercept radical species with chloroform gave a mixture of $Cp^*IrPPh_3Cl_2$ and $Cp^*IrPPh_3(H)(Cl)$, an ambiguous result since chloroform routinely reacts with iridium hydrides in this series to form chlorides. However, in contrast to the experimental observation, recombination of the radical pair (k_{-1} step) is expected to be much faster than its reaction with PPh_3 (k_2 step) at these concentrations of PPh_3.

The intermediate $(C_5Me_4CH_2)Ir(PPh_3)H$ (F) formed by reversible deprotonation of Cp* by ethoxide could, on binding PPh_3 and migration of the metal hydride to the fulvene, give the observed products. Several experiments rule out this pathway. It predicts that the ethanol hydroxyl proton formed from **3** is derived from Cp*, not Ir–H. The ethoxy deuteride **3**-d_1, however, forms ethanol-d_1 on treatment with phosphine. Quantitative identification of the ethanol proved difficult, but other experiments also argue against this mechanism. If intermediate F is in equilibrium with ethanol, it should react with EtOD to give incorporation of D in the Cp* ring methyl groups; this result is not observed when **3** is stirred in EtOD for 1 week. Alternatively, deprotonation of the Cp* methyl group by ethoxide could be caused by binding of phosphine; then the above chemistry would occur after the rate-determining step. As a direct test of the feasibility of Cp* deprotonation under these conditions, the complex $Cp^*Ir(PPh_3)_2D^+BF_4^-$ (**17b**) was prepared by protonation of $Cp^*Ir(PPh_3)_2$ with D_2SO_4 followed by ion exchange. This cation was deprotonated by ethoxide anion to give $Cp^*Ir(PPh_3)_2$ (**17**), which showed no incorporation of deuterium into the Cp* ligand.

(42) Benfield, F. W. S.; Green, M. L. H. *J. Chem. Soc., Dalton Trans.* **1974**, 1324.

Heterolytic cleavage of the iridium–oxygen bond to give ion pair G is an attractive proposal, especially since Atwood and co-workers have provided evidence that dissociation of alkoxide from an 18-electron Ir center occurs in the carbonylation of *trans*-$(PPh_3)_2Ir(CO)(OR)$.[7a] Initial ethoxide dissociation followed by phosphine coordination would give the cation $[Cp^*Ir(PPh_3)_2H]^+$, whose metal hydride could be removed by counterion ethoxide to give products. Consistent with this hypothesis, the proposed deprotonation step could be independently observed. Protonation of the metal base[43] $Cp^*Ir(PPh_3)_2$ (**17**) with HBF_4 affords the salt $[Cp^*Ir(PPh_3)_2H]^+BF_4^-$ (**17a**). This cation is rapidly deprotonated by sodium ethoxide in acetone to give ethanol and the bis(phosphine) complex **17**. As in the case of radical pair G, however, it is unlikely that trapping of the ion pair with modest concentrations of PPh_3 would be competitive in rate with ion-pair recombination.

To test for the intermediacy of the ion pair G in the PPh_3-induced reductive elimination of ethanol from ethoxy hydride **3**, we measured the rate of this reaction in the polar coordinating solvent DMF. Superior solvation of this charged intermediate by DMF as compared to toluene is expected to result in a greatly enhanced rate of reaction (rate enhancements of several orders of magnitude are often seen in organic systems).[44] However, the reaction proceeds only about twice as fast in DMF as in toluene, as discussed above.

In an organic system, this result would suggest that the ion pair G was not the intermediate. However, the effect of solvent on organometallic reaction rates is less well understood. Several organometallic systems believed to involve ionic intermediates exhibit only moderate rate enhancements in polar solvent. For example, the oxidative addition of methyl iodide to Vaska's complex *trans*-$(PPh_3)_2Ir(CO)Cl$ is believed to involve a transition state with considerable polar character,[45] yet in this system the reaction rate in DMF is only about 10 times greater than in toluene.[46]

The standard explanation of solvent effects assumes that the transition state is (a) more ionic than the starting material and (b) more highly solvated than the starting material. As the Ir center is sterically encumbered with bulky ligands, the ion pair may be effectively shielded from solvent. Alternatively, the ground state and the transition state might be stabilized by interaction with the solvent to a similar extent, leading to a small rate enhancement in the polar solvent. Similar solvent stabilization of the ground state and the intermediate could also explain the small solvent effect. Therefore we sought another method to test for the intervention of a charged intermediate.

As mentioned above, the oxidative addition of methyl iodide to Vaska's complex displays only a small solvent effect although it is thought to involve a polar transition state. Thompson and Sears[47] showed that variation of the triphenylphosphine ligands on Vaska's complex, however, produced large changes: the relative rates for the para-substituted triarylphosphines $P(p\text{-}XC_6H_4)_3$ are 1750, 910, 185, and 6 for X = MeO, Me, H, and F. Correlation of the observed rates with Hammett-type substituent constants developed by Tabachnik specifically for P centers was excellent; the negative slope of the Hammett plot was ascribed to the polar nature of the transition state.

(43) Werner, H. *Angew. Chem., Int. Ed. Engl.* **1983**, *22*, 927.
(44) Reichardt, C. *Solvents and Solvent Effects in Organic Chemistry*; VCH: Weinheim, 1988; pp 121–285.
(45) Chock, P. B.; Halpern, J. *J. Am. Chem. Soc.* **1966**, *88*, 3511.
(46) Stieger, H.; Kelm, H. *J. Phys. Chem.* **1973**, *77*, 290.
(47) Thompson, W. H.; Sears, C. T., Jr. *Inorg. Chem.* **1977**, *16*, 769.

As we also observed a small solvent effect, we carried out a similar study (Table V). However, in contrast to the observations made on the oxidative addition reaction, only small rate changes were observed and within the limits of measurement the substitutions had no effect. Unless the ground state and the intermediate are stabilized or destabilized to almost the same extent by each substituent, our combined data suggest that the k_1 step involves little charge separation.

The competition studies also show a small effect of arylphosphine variation, but the trend, that the less basic *p*-fluoro-substituted phosphine was a better trap for intermediate X than the more basic *p*-methoxy- or methyl-substituted ligand, seems real. If the intermediate is the ion pair $[Ir]H^+OEt^-$, then one might expect the cationic iridium center to be selectively trapped by an electron-rich (more basic) phosphine. As the opposite result (albeit small) is observed, we again conclude that postulation of such a charged intermediate is not the best explanation of the observed data.

Ring Slip. As a final mechanistic alternative, the intermediate X could be formed from **3** by a slip of the Cp* ligand from the ordinary η^5- to an η^3-bonding mode to give the unsaturated η^3-Cp*IrPPh$_3$(OEt)(H) (species H in Scheme XIII). Coordination of PPh_3 to this 16-electron intermediate followed by elimination of ethanol concomitant with return of the ring to its η^5 ligation would explain the observed kinetics.

Such ring-slipped intermediates have been previously invoked in related systems. Rerek and Basolo[48] showed that substitution of CO by phosphine in Cp'Rh(CO)$_2$ (Cp' = Cp, Cp*) proceeds by an associative mechanism, presumably via the ring-slipped η^3-Cp'Rh(CO)$_2$PR$_3$. Unlike this 18-electron species, intermediate H, η^3-Cp*IrPPh$_3$(OEt)(H), is a coordinatively unsaturated, 16-electron compound. This proposed intermediate also differs from other postulated ring-slipped species in that the ring slips without requiring a new ligand to fill the empty coordination site. This behavior may be rationalized if the coordinatively unsaturated species is stabilized by the electron-donating alkoxide or amide ligand. The stabilization of this intermediate (see Scheme XIII for an illustration) and hence the rate of ring slip should then depend on the electron-donating ability of the ligand X in Cp*IrPPh$_3$(H)(X). The observed rates OEt ~ NHCH$_2$Ph > NHPh > OPh are consistent with this argument. The formation of Cp*IrPPh$_3$(OEt)(H) from unobserved Cp*IrPPh$_3$(OEt)$_2$ may also be rationalized in this way. With two strongly donating ethoxides, ring slip could occur easily, enabling β-hydride elimination to give the observed product. Finally, this model suggests that the analogous methyl alkoxide and amide compounds Cp*IrPPh$_3$(Me)(X) will undergo a similar process to generate an open coordination site. This behavior is in fact observed.[40b]

If the ligand-induced reductive elimination actually proceeds via ring-slipped intermediate H, then ligand substitution for PPh_3 instead of elimination of alcohol or amine might occur. However, as discussed above, reaction of Cp*IrPPh$_3$(OEt)(H) with triarylphosphines PAr_3 gives cleanly Cp*Ir(PPh$_3$)(PAr_3) and ethanol; no substitution products such as Cp*IrPAr_3(OEt)(H) or Cp*Ir(PAr_3)$_2$ are observed. The same result occurs with PPh_2Me. All these reactions occur in hours at room temperature. Under these conditions, reaction of PPh_3 with Cp*IrPPh$_3$(NHPh)(H) leads slowly (days) to the formation of Cp*Ir(PPh_3)$_2$ and aniline. An identical result was obtained with PPh_2Me; Cp*Ir(PPh_3)(PPh_2Me) and aniline were formed over several days; ligand substitution was not observed.[49]

Conclusions. The Cp* iridium hydrido alkoxides and amides Cp*IrPPh$_3$(H)(OR) and Cp*IrPPH$_3$(H)(NHR) reported here can be prepared by simple metathesis reactions. They undergo insertion reactions with heterocumulenes typical of metal–oxygen and metal–nitrogen bonds. On treatment with several two-electron ligands L, these complexes form alcohol or amine, respectively, and the appropriate Cp*Ir(PPh$_3$)L. Kinetic studies suggest that the PPh_3-induced reductive eliminations proceed via a ring-slipped 16-electron intermediate η^3-Cp*IrPPh$_3$(H)(X), which is reversibly formed from the starting material and trapped by phosphine to give the observed products. This proposed coordinatively unsaturated intermediate is presumably stabilized by electron donation from the oxygen or nitrogen lone pair to the metal center. The increased kinetic stability of aryloxide and anilide vs amide and alkoxide ligands has been ascribed to greater M–O and M–N bond strengths. Since OAr and NHAr are softer ligands than OR and NHR, they enjoy more favorable bonding interactions with the soft metal center. The hard ligands may be more reactive for another reason: they can stabilize coordinatively unsaturated metal centers.

Experimental Section

General Considerations. Unless otherwise noted, all reactions and manipulations were performed in dry glassware under nitrogen atmosphere in a Vacuum Atmospheres 553-2 drybox equipped with an M6-40-1H Dri-train or by using standard Schlenk techniques.

All ^1H, ^2H, ^{13}C, and ^{31}P NMR spectra were recorded on 300-, 400-, or 500-MHz instruments at the University of California, Berkeley NMR facility. The 300-MHz instrument was constructed by Rudi Nunlist and interfaced with a Nicolet 1280 computer. The 400- and 500-MHz machines were commercial Bruker AM series spectrometers. ^1H and ^{13}C NMR chemical shifts are reported in parts per million downfield from tetramethylsilane. ^{31}P NMR chemical shifts are given in parts per million downfield from 85% H_3PO_4. Coupling constants are given in hertz. Infrared spectra were recorded on a Perkin-Elmer Model 1550 Fourier transform spectrometer. Infrared bands are reported in inverse centimeters. Melting points are uncorrected and were determined with a Thomas-Hoover Unimelt capillary melting-point apparatus. Elemental analyses were conducted by the UC Berkeley Microanalysis Facility, and mass spectra were recorded by the UC Berkeley Mass Spectrometry laboratory on AEI-MS12 and Kratos MS-50 instruments.

Benzene, toluene, and THF were distilled from sodium/benzophenone. Pentane was distilled from lithium aluminum hydride. Alcohols ROH were distilled from the corresponding Mg(OR)$_2$ salts. Isocyanates and *tert*-butyl isocyanide were distilled from phosphorus pentoxide. Phenyl acetate, carbon disulfide, and hexamethyldisiloxane were distilled from calcium hydride. Maleic anhydride was recrystallized from chloroform. Succinic anhydride was recrystallized from acetone. Aniline was distilled from calcium hydride; benzylamine, from sodium metal. Triphenylphosphine was recrystallized from pentane. Diphenylmethylphosphine was distilled from sodium. Trityllithium was prepared from Ph_3CH and butyllithium in toluene/THF and isolated as an orange powder, which was stored at −40 °C. [Cp*IrCl$_2$]$_2$ and Cp*IrPPh$_3$Cl$_2$ were prepared by literature methods.[50] Cp*Ir(PPh_2Me)Cl$_2$ was prepared from [Cp*IrCl$_2$]$_2$ and PPh_2Me in CH_2Cl_2; experimental details are given in ref 40b. Unless otherwise noted, all other reagents were used as received

(48) Rerek, M. E.; Basolo, F. *J. Am. Chem. Soc.* **1984**, *106*, 5908.

(49) After several days, the initial product Cp*IrPPh$_3$(PPh_2Me) undergoes ligand substitution to give Cp*Ir(PPh_2Me)$_2$ and PPh_3. This was confirmed in a control experiment, and Cp*Ir(PPh_2Me)$_2$ was prepared and characterized independently (see Experimental Section).

(50) (a) Ball, R. G.; Graham, W. A. G.; Heinekey, D. M.; Hoyano, J. K.; McMaster, A. D.; Mattson, B. M.; Michel, S. T. *Inorg. Chem.* **1990**, *29*, 2023. (b) Kang, J. W.; Moseley, K.; Maitlis, P. M. *J. Am. Chem. Soc.* **1969**, *91*, 5970.

Table IX. NMR Data for Alkoxy and Amido Hydride $Cp^*IrPPh_3(H)(X)$ Compounds[a]

compd	δ	mult	J, Hz	assgnt	integral	compd	δ	mult	J, Hz	assgnt	integral
				(a) ^1H NMR							
3 (X = OEt)	7.7–7.9	m		P*Ph*$_3$	6	**6e** (X = OPh)	7.8	m		P*Ph*$_3$	6
	7.0–7.1	m		P*Ph*$_3$	9		7.4	m		O*Ph*	2
	3.79	d quintets	9.0, 6.0	OC*H*$_2$CH$_3$	2		7.0	m		P*Ph*$_3$, O*Ph*	11
	1.59	d	1.8	C$_5$*Me*$_5$	15		6.8	m		O*Ph*	1
	1.20	t	6.0	OCH$_2$C*H*$_3$	3		1.43	d	2.0	C$_5$*Me*$_5$	15
	−13.20	d	37.7	Ir*H*	1		−12.02	d	38.9	Ir*H*	1
6b (X = O-*n*-Pr)	7.7–7.9	m		P*Ph*$_3$	6	**8a** (X = NHPh)[b]	7.39–7.29	m		P*Ph*$_3$	15
	7.0–7.1	m		P*Ph*$_3$	9		6.61	t	7.5	NH*Ph*	2
	3.76	dd	9.0, 5.0	OC*H*$_2$	1		6.19	d	7.7	NH*Ph*	2
	3.43	dd	9.0, 5.0	OC*H*$_2$	1		5.84	t	7.1	NH*Ph*	1
	1.59			C$_5$*Me*$_5$	15		1.64	d	1.1	C$_5$*Me*$_5$	15
	1.41	m		OCH$_2$C*H*$_2$	2		1.24	d	4.2	N*H*	1
	0.92	t	7.0	C*H*$_3$	3		−14.33	d	36.8	Ir*H*	1
	−13.29	d	37.4	Ir*H*	1	**8b** (X = NHCH$_2$Ph)	7.62–7.56	m		*Ph*	19 (totl)
6c (X = O-*i*-Pr)	7.8–7.9	m		P*Ph*$_3$	6		7.21–7.17	m		*Ph*	
	7.01–7.1	m		P*Ph*$_3$	9		7.05–7.01	m		*Ph*	
	2.86	m		OC*H*	1		3.90–3.79	m		C*H*$_2$Ph	2
	1.55	d	2.1	C$_5$*Me*$_5$	15		1.68			C$_5$*Me*$_5$	15
	1.20	d	5.8	OCH*Me*	3		0.18	br		N*H*	1
	0.87	d	5.9	OCH*Me*	3		−15.77	d	36.4	Ir*H*	1
	−13.45	d	37.1	Ir*H*	1						
6d (X = OEt)·(PhOH)	11.8	v br		PhO*H*	1						
	7.6–7.8	m		*Ph*	25 (totl)						
	7.0–7.2	m		*Ph*							
	6.7–6.9	m		*Ph*							
	3.6	m		OC*H*$_2$	2						
	1.54			C$_5$*Me*$_5$	15						
	1.01	t	6.9	C*H*$_3$	3						
	−12.86	d	37.7	Ir*H*	1						
				(b) $^{13}C\{^1H\}$ NMR							
3 (X = OEt)	135.6	d	54.0	ipso P*Ph*$_3$		**8a** (X = NHPh)[b]	159.8			ipso N*Ph*	
	134.4	d	10.3	o or m P*Ph*$_3$			135.7	d	54.5	ipso P*Ph*$_3$	
	129.4			P*Ph*$_3$			134.7	d	10.5	o or m P*Ph*$_3$	
	128.1			P*Ph*$_3$			130.4			p P*Ph*$_3$	
	91.4			C$_5$Me$_5$			128.6	d	10.0	o or m P*Ph*$_3$	
	75.3			OCH$_2$			128.3			N*Ph*	
	23.9			CH$_3$			117.5			N*Ph*	
	9.7			C$_5$*Me*$_5$			110.1			N*Ph*	
6b (X = O-*n*-Pr)	135.7	d	52.6	ipso P*Ph*$_3$			93.5	d	3.2	C$_5$Me$_5$	
	134.4	d	16.9	o or m P*Ph*$_3$			9.9			C$_5$*Me*$_5$	
	129.4			P*Ph*$_3$		**8b** (X = NHCH$_2$Ph)[b]	149.7			ipso CH$_2$*Ph*	
	127.8			P*Ph*$_3$			136.1	d	52.9	ipso P*Ph*$_3$	
	91.5			C$_5$Me$_5$			134.6	d	10.5	o or m P*Ph*$_3$	
	82.9			OCH$_2$			130.1			*Ph*	
	31.3			CH$_2$			129.0			*Ph*	
	11.5			CH$_3$			128.39	d	9.8	o or m P*Ph*$_3$[c]	
	9.4			C$_5$*Me*$_5$			128.46			*Ph*[c]	
6c (X = O-*i*-Pr)	135.4	d	53.5	ipso P*Ph*$_3$			128.40			*Ph*[c]	
	134.6	d	10.2	o or m P*Ph*$_3$			127.9			*Ph*	
	129.4			P*Ph*$_3$			125.5			*Ph*	
	127.6			P*Ph*$_3$			93.7	d	3.0	C$_5$Me$_5$	
	91.2			C$_5$Me$_5$			68.8			CH$_2$Ph	
	76.8			OCH$_2$			9.7			C$_5$*Me*$_5$	
	28.0			CH$_3$							
	27.5			CH$_3$							
	9.8			C$_5$*Me*$_5$							
6e (X = OPh)	170.2			ipso O*Ph*							
	134.8	d	54.4	ipso P*Ph*$_3$							
	134.4			P*Ph*$_3$							
	134.0			P*Ph*$_3$							
	129.8			P*Ph*$_3$							
	121.8			O*Ph*							
	121.6			O*Ph*							
	113.9			O*Ph*							
	91.8			C$_5$Me$_5$							
	9.7			C$_5$*Me*$_5$							

[a] All spectra in C_6D_6 at 20 °C unless indicated. [b] THF-d_8. [c] Overlapping peaks.

from commercial suppliers. Reactions with gases involved condensation of a calculated pressure (ideal gas law) of gas from a bulb of known volume into the reaction vessel at −196 °C. Unless noted otherwise, all reactions were done at ambient temperature.

Kinetics. All kinetics experiments were monitored by ultraviolet–visible spectroscopy using a Hewlett-Packard 8450A instrument equipped with a 89100A temperature controller. Standard solutions were prepared in the drybox in volumetric flasks and stored in the drybox freezer at −40 °C. Individual runs were prepared in the drybox by transferring aliquots of cold standard solutions using volumetric pipets into a quartz cuvette, which was then sealed with a Kontes high-vacuum stopcock,

Table X. NMR Data for Cp*IrPPh$_3$(H)(X) Compounds[a]

compd	δ	mult	*J*, Hz	assgnt	integral	compd	δ	mult	*J*, Hz	assgnt	integral
				(a) ^{1}H NMR							
7a (X = $O_2CCH{=}CHCO_2Et$)	7.79–7.73	m		P*Ph*$_3$	6	**11b** (X = *p*-TolNCO$_2$Et)	7.8–7.9	m		*Ph*	6
	7.08–7.00	m		P*Ph*$_3$	9		7.0–7.1	m		*Ph*	13
	5.57–5.47	m		C*H*	2		3.7–4.0	dm		OC*H*$_2$	2
	4.12–4.04	m		OC*H*$_2$	2		2.21			PhC*H*$_3$	3
	1.66			C$_5$*Me*$_5$	15		1.50	d	1.7	C$_5$*Me*$_5$	15
	1.02	t	6.8	OCH$_2$C*H*$_3$	3		0.92	t	7.0	C*H*$_3$	3
	−12.38	d	37.7	Ir*H*	1		−14.96	d	37.9	Ir*H*	1
7b (X = $O_2CCH_2CH_2CO_2Et$)	7.79–7.73	m		P*Ph*$_3$	6	**11c** (X = MeNCO$_2$Et)	7.8–7.9	m		P*Ph*$_3$	6
	7.09–7.00	m		P*Ph*$_3$	9		7.0–7.1	m		P*Ph*$_3$	9
	3.95	q	7.1	OC*H*$_2$	2		3.8–4.1	dm		OC*H*$_2$	2
	2.51–2.48	m		C*H*$_2$	2		3.31			N*Me*	3
	2.32–2.14	m		C*H*$_2$	2		1.63	d	1.6	C$_5$*Me*$_5$	15
	1.57	d	1.5	C$_5$*Me*$_5$	15		0.97	t	6.9	C*H*$_3$	3
	0.95	t	7.0	C*H*$_3$	3		−15.54	d	36.8	Ir*H*	1
	−12.54	d	37.9	Ir*H*	1	**12a** (X = S_2CNHPh)	11.20			N*H*	1
9 (X = OCO$_2$Et)	7.8–7.9	m		P*Ph*$_3$	6		8.32	d	8.0	*Ph*	20 (totl)
	7.1–7.2	m		P*Ph*$_3$	9		7.46	m		*Ph*	
	3.89	m		OC*H*$_2$	2		7.24	m		*Ph*	
	1.59			C$_5$*Me*$_5$	15		6.96	m		*Ph*	
	1.03	t	6.9	C*H*$_3$	3		1.42	d	1.2	C$_5$*Me*$_5$	15
	−12.09	d	38.2	Ir*H*	1		−14.99	d	34.6	Ir*H*	1
10 (X = S_2COEt)	7.5–7.7	m		P*Ph*$_3$	6	**12b** (X = S_2CNHCH_2Ph)[b]	9.23			N*H*	1
	7.0–7.1	m		P*Ph*$_3$	9		7.37–7.33	br		*Ph*	20
	4.7	ddq		OC*H*$_2$	2		5.03–4.69	dm		C*H*$_2$Ph	2
	1.56	d	1.7	C$_5$*Me*$_5$	15		1.55			C$_5$*Me*$_5$	15
	1.17	t	6.9	C*H*$_3$	3		−15.37	d	33.7	Ir*H*	1
	−13.79	d	34.3	Ir*H*	1	**13b** (X = NPhCONHMe)	7.95–7.89	m			20 (totl)
11a (X = PhNCO$_2$Et)	7.7–7.9	m		P*Ph*$_3$	6		7.29–7.27	m			
	7.0–7.1	m		*Ph*	14		7.12–6.99	m			
	3.7–4.0	dm		OC*H*$_2$	2		6.77	m			
	1.48	d	1.8	C$_5$*Me*$_5$	15		3.60	br		N*H*	1
	0.90	t	7.0	C*H*$_3$	3		2.34	d	4.4	N*Me*	3
	−14.95	d	38.0	Ir*H*	1		1.51			C$_5$*Me*$_5$	15
							−15.00	d	37.4	Ir*H*	1
				(b) ^{13}C{^{1}H} NMR							
7a (X = $O_2CCH{=}CHCO_2Et$)	172.0			*CO*		**11b** (X = *p*-TolNCO$_2$Et)[b]	159.1			*CO*	
	166.3			*CO*			153.3			ipso N*Ar*	
	136.4			*CH*=CH			135.3	d	50.6	ipso P*Ph*$_3$[c]	
	134.4	d	57.3	ipso P*Ph*$_3$			134.9	d	10.6	o or m P*Ph*$_3$[c]	
	134.9	d	10.8	o or m P*Ph*$_3$			130.1	d	1.6	*Ph*	
	129.8			*Ph*			129.8			*Ph*	
	127.8			*Ph*[d]			128.3			*Ph*	
	122.2			*CH*=CH			127.7	d	10.1	o or m P*Ph*$_3$	
	92.4	d	2.6	C$_5$Me$_5$			127.3			*Ph*	
	59.8			OCH$_2$			93.2			*C*$_5$Me$_5$	
	14.4			*CH*$_3$			60.2			OCH$_2$	
	10.2			C$_5$*Me*$_5$			20.7			PhCH$_3$	
7b (X = $O_2CCH_2CH_2CO_2Et$)	178.2			*CO*			15.4			OCH$_2$CH$_3$	
	173.3			*CO*			9.8			C$_5$*Me*$_5$	
	134.7	d	54.0	ipso P*Ph*$_3$		**12a** (X = S_2CNHPh)[b]	201.0	br m		*CS*$_2$	
	134.9	d	10.6	o or m P*Ph*$_3$			141.27			*Ph*[d]	
	129.8			*Ph*			141.15			*Ph*[d]	
	127.9			*Ph*[d]			134.41			ipso P*Ph*$_3$[c]	
	91.9	d	2.5	*C*$_5$Me$_5$			134.00	d	10.4	o or m P*Ph*$_3$[c]	
	59.6			OCH$_2$			130.6	d	2.2	p P*Ph*$_3$	
	31.7			*CH*$_2$			128.9			*Ph*	
	31.0			*CH*$_2$			128.4	d	10.4	o or m P*Ph*$_3$	
	14.4			OCH$_2$CH$_3$			125.02			*Ph*	
	10.0			C$_5$*Me*$_5$			124.99			*Ph*	
10 (X = S_2COEt)	224.1			*CS*$_2$			122.30			*Ph*	
	135.1	d	56.2	ipso P*Ph*$_3$			122.15			*Ph*	
	134.2			*Ph*			95.8	d	1.8	*C*$_5$Me$_5$	
	130.0			*Ph*			9.4			C$_5$*Me*$_5$	
	127.9			*Ph*		**12b** (X = S_2CNHCH_2Ph)[b]	201.6			*CS*$_2$	
	95.0			*C*$_5$Me$_5$			138.6			ipso CH$_2$*Ph*	
	69.5			OCH$_2$			134.2	d	56.3	ipso P*Ph*$_3$[c]	
	14.6			*CH*$_3$			133.9	d	10.3	o or m P*Ph*$_3$[c]	
	9.3			C$_5$*Me*$_5$			130.4			*Ph*	
11a (X = PhNCO$_2$Et)	158.8			*CO*			128.9			*Ph*	
	155.1			ipso N*Ph*			128.33			*Ph*[e]	
	135.6	d	53.4	ipso P*Ph*$_3$			128.26	d	10.2	o or m P*Ph*$_3$[c]	
	135.2	d	10.1	o or m P*Ph*$_3$			127.65			*Ph*	
	129.5			*Ph*			95.4	d	2.2	*C*$_5$Me$_5$	
	128.9			*Ph*			51.4			CH$_2$Ph	
	128.5			*Ph*			9.2			C$_5$*Me*$_5$	
	127.6			*Ph*		**13b** (X = NPhCONHMe)[c]	162.6			*CO*	
	126.9			*Ph*			156.2			ipso N*Ph*	
	93.0	d	3.2	*C*$_5$Me$_5$			136.3	d	53.8	ipso P*Ph*$_3$[c]	
	60.3			OCH$_2$			135.8	d	10.2	o or m P*Ph*$_3$[c]	
	15.3			*CH*$_3$			129.9			*Ph*	
	9.7			C$_5$*Me*$_5$			129.4			*Ph*	

Table X (*Continued*)

compd	δ	mult	*J*, Hz	assgnt	integral
13b (X = NPhCONHMe)[c]	127.9	d	10.1	o or m P*Ph*$_3$[e]	
	127.8			*Ph*[e]	
	120.1			*Ph*	
	93.5	d	2.0	C$_5$*Me*$_5$	
	28.9			N*Me*	
	9.9			C$_5$*Me*$_5$	

[a] All spectra in C_6D_6 at 20 °C unless indicated. [b] CD_2Cl_2. [c] THF-d_8. [d] $CDCl_3$. [e] Overlapping peaks. [f] Partially obscured by solvent. [g] Quaternary according to DEPT experiments.

Table XI. NMR Data for Cp*Ir(PPh$_3$)L Compounds[a]

compd	δ	mult	*J*, Hz	assign	integral
		(a) ^{1}H NMR			
14 (L = CO)	7.7–7.9	m		P*Ph*$_3$	6
	7.0–7.1	m		P*Ph*$_3$	9
	1.79			C$_5$*Me*$_5$	15
15 (L = C_2H_4)	7.8–7.6	m		P*Ph*$_3$	6
	7.2–7.0	m		P*Ph*$_3$	9
	1.61	d	1.5	C$_5$*Me*$_5$	15
	1.10–1.09	m		C_2H_4	4
16 (L = CN-*t*-Bu)	7.9–8.0	m		P*Ph*$_3$	6
	7.1–7.2	m		P*Ph*$_3$	9
	1.94	d	1.3	C$_5$*Me*$_5$	15
	1.01			*t-Bu*	9
17 (L = PPh_3)	7.71	m		P*Ph*$_3$	12
	6.92	m		P*Ph*$_3$	18
	1.56	t	1.3	C$_5$*Me*$_5$	15
18 (L = PPh_2Me)	8.0–7.9	m		*Ph*	25 (totl)
	7.7–7.6	m		*Ph*	
	7.2–7.1	m		*Ph*	
	7.0–6.9	m		*Ph*	
	1.57			C$_5$*Me*$_5$	15
	1.23	d	8.0	P*Me*	3
		(b) ^{13}C{^{1}H} NMR			
14 (L = CO)	181.6	d	15.1	*C*O	
	136.6	d	56.0	ipso P*Ph*$_3$	
	134.3	d	11.9	o or m P*Ph*$_3$	
	129.5			P*Ph*$_3$	
	127.7			P*Ph*$_3$	
	94.6			*C*$_5$Me$_5$	
	10.5			C$_5$*Me*$_5$	
15 (L = C_2H_4)	135.1	d	46.3	ipso P*Ph*$_3$	
	134.9	d	10.3	o or m P*Ph*$_3$	
	129.0			p P*Ph*$_3$	
	127.3	d	10.0	o or m P*Ph*$_3$	
	91.2			*C*$_5$Me$_5$	
	14.6			*C*$_2$H$_4$	
	9.6			C$_5$*Me*$_5$	
16 (L = *t*-BuNC)	179.9	d	16.6	*t*-Bu*NC*	
	137.7	d	51.3	ipso P*Ph*$_3$	
	134.7	d	11.6	o or m P*Ph*$_3$	
	128.9			p P*Ph*$_3$	
	127.4	d	10.1	o or m P*Ph*$_3$	
	93.1	d	3.2	*C*$_5$Me$_5$	
	52.0			*C*Me$_3$	
	31.8			*C*Me$_3$	
	10.9			C$_5$*Me*$_5$	
17 (L = PPh_3)	139.4	virtual t	24.0	P*Ph*$_3$	
	135.3	virtual t	5.5	P*Ph*$_3$	
	126.7	virtual t	4.6	P*Ph*$_3$	
	128.1			P*Ph*$_3$	
	93.0			*C*$_5$Me$_5$	
	10.6			C$_5$*Me*$_5$	
18 (L = PPh_2Me)[b]	140.7	d	45.5	ipso P*Ph*$_3$	
	139.5	d	46.3	ipso P*Ph*$_3$	
	135.3	d	11.6	o or m P*Ph*$_3$	
	133.1	d	11.4	o or m P*Ph*$_3$	
	128.5			p P*Ph*$_3$	
	128.2			p P*Ph*$_3$	
	127.2	d	9.7	o or m P*Ph*$_3$	
	127.0	d	9.7	o or m P*Ph*$_3$	
	92.5			*C*$_5$Me$_5$	
	20.3	d	35.8	P*Me*	
	10.1			C$_5$*Me*$_5$	

[a] All spectra in C_6D_6 at 20 °C unless indicated. [b] CD_2Cl_2.

removed from the box, and placed in the spectrometer. The cuvette was allowed to reach temperature equilibrium with the cell holder before data were acquired. The solution in the cell was stirred with a micro stir bar, and a stream of nitrogen was passed through the cell holder to prevent condensation of water onto the cell surface.

Reactions were generally monitored by observing the growth of absorbance due to product over time. The reaction of Cp*IrPPh$_3$(OEt)(H) with PPh_3 was observed at 355 nm. The reaction of Cp*IrPPh$_3$(NHCH$_2$Ph)(H) with PPh_3 was watched at 355 nm, and that of Cp*IrPPh$_3$(NHPh)(H) with PPh_3 at 500 nm. Runs with Cp*IrPPh$_3$(OEt)(D) and of Cp*IrPPh$_3$(OEt)(H) in DMF were monitored at 355 nm, as were all reactions using triarylphosphine complexes Cp*IrPAr$_3$(OEt)(H). In all cases reactions were observed for at least 3 half-lives. Exposure of solutions to room light for varying periods of time had no effect on the measured rates.

Plots of absorbance vs time were fit by using the NEGINF program by Eric Wasserman of these laboratories to the increasing exponential function $y = A_1(1 - \exp(-A_2x)) + A_3$, where y = absorbance and x = time. From the least-squares fits, the observed rate is A_2 and the infinity point is $A_1 + A_3$.

Cp*IrPPh$_3$(OEt)(H) (3). Freshly distilled ethanol (50 mL) was vacuum-transferred into a flask containing orange Cp*IrPPh$_3$Cl$_2$ (943 mg, 1.43 mmol) and NaOEt (220 mg, 3.24 mmol). The resulting orange slurry was stirred for 3 h, after which time the mixture was yellow. The ethanol was removed in vacuo. (This can also be done after longer reaction times (~18 h) without loss of yield.) The remaining yellow oil was extracted with pentane and filtered through a frit. The clear yellow filtrate was concentrated and cooled to −40 °C to afford a yellow solid (779 mg, 86%, in two crops): mp 95–97 °C dec; ^{31}P{^{1}H} NMR (C_6D_6) δ 16.6; IR (C_6D_6) 2035, 1480, 1435, 1360, 1110, 1095, 1045, 692 cm^{-1}. Anal. Calcd for $C_{30}H_{36}IrOP$: C, 56.67; H, 5.71. Found: C, 56.46; H, 5.86.

Cp*IrPPh$_3$(OCD$_2$CH$_3$)D (3-*d*$_3$) and Cp*IrPPh$_3$(OEt)(D) (3-*d*$_1$). (a) A mixture of Cp*IrPPh$_3$Cl$_2$ (21 mg, 3.2 × 10^{-2} mmol) and NaOCD$_2$CH$_3$ (4 mg, 5.5 × 10^{-2} mmol) in CH$_3$CD$_2$OH (5 mL) was stirred at 0 °C overnight. ^{1}H and ^{2}H NMR analysis then showed that Cp*IrPPh$_3$(OCD$_2$CH$_3$)(D) formed: ^{1}H NMR (C_6D_6) δ 7.7–7.9 (m, 6 H), 7.0–7.1 (m, 9 H), 1.59 (15 H), 1.04 (3 H); ^{2}H NMR (C_6H_6) δ 3.71–3.44 (m), 1.55. Stirring this material in EtOH overnight gave Cp*IrPPh$_3$(OEt)(D): ^{2}H NMR (C_6H_6) δ 1.56 (~5% D incorporated), −13.32 (d, J = 28.8 Hz); IR (KBr) 2956, 2910, 1482 (Ir–D), 1435, 1097, 540 cm^{-1}. (b) A 10-mL aliquot of CD$_3$CD$_2$OD was condensed into a flask containing Cp*IrPPh$_3$Cl$_2$ (99 mg, 0.15 mmol), NaOCD$_2$CD$_3$ (25 mg, 0.34 mmol), and a stir bar. The orange slurry was stirred for 2 h at which time it had become homogenous and yellow. The ethanol was removed by vacuum transfer. The yellow oil remaining was extracted with pentane and filtered through a frit. The pentane was removed in vacuo to give a yellow foam of Cp*IrPPh$_3$(OCD$_2$CD$_3$)(D) (3-*d*$_6$). Ethanol (10 mL) was condensed onto the foam and the yellow solution stirred for 7 h. Removing the solvent in vacuo gave a yellow oil, which was recrystallized from hexane at −40 °C to give 39 mg (41%) of yellow powder: ^{2}H NMR (C_6H_6) δ −13.2 (Ir–D), 1.55 (C$_5$Me$_5$; integration of the ^{1}H and ^{2}H NMR spectra suggests ~5–10% incorporation of deuterium in the Cp* methyl groups); IR (KBr) 1482 cm^{-1} (Ir–D).

Cp*IrPPh$_3$(OCD$_2$CD$_3$)(H) (6a). Ethanol-d_6 (0.5 mL) was condensed at −196 °C onto solid **3** (15 mg, 2.36 × 10^{-2} mmol). The mixture was allowed to thaw and the yellow solution stirred overnight. The volatile materials were removed by distillation to afford a yellow solid: ^{1}H NMR (C_6D_6) δ 7.7–7.9 (m, 6 H), 7.0–7.1 (m, 9 H), 1.60 (s, 15 H), −13.20 (d, J = 37.7 Hz, 1 H); ^{2}H NMR (C_6H_6) δ 3.70 (m, 2 H), 0.97 (m, 3 H).

Cp*IrPPh$_3$(O-*n*-Pr)(H) (6b). 1-Propanol (50 mL) was condensed at −196 °C into a flask containing **3** (80.0 mg, 1.26 × 10^{-1}

mmol). The mixture was stirred overnight, and the solvent was evaporated under vacuum to give a yellow oil. This was extracted with THF (2 × 50 mL), and the solvent was removed in vacuo to remove remaining 1-propanol. Crystallization from pentane at −40 °C gave 59 mg of yellow microcrystals (72%): $^{31}P\{^1H\}$ NMR (C_6D_6) δ 14.3; IR (C_6D_6) 2081, 1482, 1374, 1112, 1097, 1069, 815, 809, 698 cm^{-1}. Anal. Calcd for $C_{31}H_{38}IrOP$: C, 57.29; H, 5.91. Found: C. 57.31; H, 6.07.

Cp*IrPPh$_3$(O-*i*-Pr)(H) (6c). A solution of **3** (104 mg, 1.64 × 10^{-1} mmol) in 2-propanol (20 mL) was stirred overnight. After removal of the solvent under vacuum, ^1H NMR analysis showed 80% conversion to the desired product. Repeating this procedure two times with fresh 2-propanol gave 100% conversion. Residual 2-propanol was removed by dissolving the yellow powder in THF (3 × 20 mL) and removing the solvents under vacuum. Crystallization from toluene/pentane at −40 °C gave yellow crystals (89.3 mg, 84%): $^{31}P\{^1H\}$ NMR (C_6D_6) δ 16.4; IR (C_6D_6) 2900, 2080, 1430, 1130, 1090, 1030, 750, 700 cm^{-1}. Anal. Calcd for $C_{31}H_{38}IrOP$: C, 57.30; H, 5.89. Found: C, 57.16; H, 6.10.

Single Crystal X-ray Diffraction Study of 6c. This study was carried out by Dr. F. J. Hollander of the UC Berkeley X-ray Diffraction Facility (CHEXRAY). Pale yellow prismatic crystals of **6c** were obtained by slow crystallization from toluene/pentane at −40 °C. Fragments cleaved from some of these crystals were mounted on glass fibers by using polycyanoacrylate cement. After mounting, the fragments were coated with the cement to isolate them from the atmosphere. Precession photographs indicated monoclinic Laue symmetry and yielded preliminary cell dimensions. Systematic absences were consistent only with the space group $P2_1/c$.

The crystal used for data collection was then transferred to an Enraf-Nonius CAD-4 diffractometer and centered in the beam. Automatic peak search and indexing procedures yielded the monoclinic reduced primitive cell. The final cell parameters and specific data collection parameters are given in Table Ia.

The 4063 raw intensity data were converted to structure factor amplitudes and their esd's by correction for scan speed, background, and Lorentz and polarization effects. Inspection of the intensity standards showed a monotonic isotropic decrease to 0.93 of the original intensity. The data were corrected for this decay. Inspection of the azimuthal scan data showed a variation I_{min}/I_{max} = 0.94 for the average curve. An empirical correction for absorption, based on the azimuthal scan data, was applied to the intensities, since the faces of the crystal were poorly defined. Removal of systematically absent and redundant data left 3642 unique data.

The structure was solved by Patterson methods and refined via standard least-squares and Fourier techniques. In a difference Fourier map calculated following refinement of all non-hydrogen atoms with anisotropic thermal parameters, peaks corresponding to the expected positions of all the hydrogen atoms were found. With the exception of the hydrogen attached to iridium, hydrogens were included in the structure factor calculations in their expected positions based on idealized bonding geometry but were not refined in least squares. They were assigned isotropic thermal parameters 1–2 Å^2 larger than the equivalent B_{iso} of the atom to which they were bonded. A secondary extinction parameter was refined in the final cycles of least squares. The final residuals for 312 variables refined against the 2979 data for which $F^2 > 3\sigma(F^2)$ were R = 1.59%, R_w = 2.08%, and GOF = 1.378. The R value for all 3642 data was 2.98%.

The quantity minimized by the least-squares program was $w(F_o - F_c)^2$, where w is the weight of a given observation. The p factor, used to reduce the weight of intense reflections, was set to 0.02 in the final stages of the refinement. The analytical forms of the scattering factor tables for the neutral atoms were used, and all non-hydrogen scattering factors were corrected for both the real and the imaginary components of anomalous dispersion.

Inspection of the residuals ordered in ranges of $(\sin\theta)/\lambda$, F_{io}, and parity and value of the individual indexes showed no unusual features or trends. The largest peak in the final difference Fourier map had an electron density of 0.48 e/Å^3. The top three peaks were all located near the iridium atom.

Cp*IrPPh$_3$(OPh)(H) (6e). A precooled (−40 °C) solution of phenol (15.0 mg, 1.59 × 10^{-1} mmol) in pentane (10 mL) was added dropwise to a cold (−40 °C) solution of **3** (101.0 mg, 1.59 × 10^{-1} mmol). The solvent was removed under vacuum immediately, leaving hydrogen-bonded adduct **6d** as a yellow solid. A solution of **6d** in 30 mL of benzene was heated to 55 °C for 1 h. Removal of the solvent under vacuum and recrystallization from toluene/pentane at −40 °C gave 97.6 mg (90%) of yellow powder **6e**: $^{31}P\{^1H\}$ NMR (C_6D_6) δ 16.5; IR (KBr) 2110, 1585, 1475, 1435, 1281, 697, 538 cm^{-1}. Anal. Calcd for $C_{34}H_{36}IrOP$: C, 59.72; H, 5.31. Found: C, 59.43; H, 5.44.

Transesterification. Phenyl acetate (15 μL, 1.18 × 10^{-1} mmol) was added to a solution of **3** (50 mg, 7.87 × 10^{-2} mmol) in 10 mL of toluene in a glass bomb. After 2 weeks, the solution had become orange-yellow. The volatile materials were distilled away, and the remaining yellow solid was recrystallized from toluene/pentane at −40 °C to afford 23 mg (43%) of yellow crystals of **6e**, whose ^1H NMR spectrum (C_6D_6) and IR spectrum (KBr) were identical with those of an authentic sample made by treatment of **3** with phenol. In a separate experiment done on twice the scale, a crude yield of 95 mg of **6e** (88%) was obtained; GC analysis of the volatile materials from this reaction (integration vs a standard of cyclohexane) demonstrated the formation of ethyl acetate in 89% yield.

Formation of Cp*IrPPh$_3$(Cl)(H) (4) from 3. (a) HCl. A solution of HCl in diethyl ether (1.24 mL of 0.0237 N solution, 2.94 × 10^{-2} mmol) was added by syringe to a toluene solution of **3** (17 mg, 2.67 × 10^{-2} mmol). The solvents were distilled off; GC analysis confirmed the formation of ethanol. The remaining yellow solid (16.2 mg, 97%) was identified by its ^1H NMR spectrum (C_6D_6), which was identical with that of an authentic sample synthesized by the literature method.[11]

(b) LiCl. A solution of **3** (11.8 mg, 1.86 × 10^{-2} mmol) in THF was added to a slurry of 1.8 mg of LiCl (4.25 × 10^{-2} mmol) in THF, and the mixture was stirred for 3 days. The THF was removed in vacuo, and the yellow solid was extracted with benzene, which was evaporated to yield 8.6 mg (74%) of Cp*IrPPh$_3$(Cl)(H), which was again identified by its ^1H NMR spectrum.

Cp*IrPPh$_3$[OC(O)CH=CHCO$_2$Et](H) (7a). A clear solution of maleic anhydride (15 mg, 0.153 mmol) in 5 mL of toluene was added dropwise to a yellow solution of 90 mg (0.142 mmol) of **3** in 10 mL of toluene. The yellow color intensified. After stirring for 40 min, the solvent was removed in vacuo to give a yellow-orange oil. Recrystallization from pentane at −40 °C afforded 78 mg (75%) of yellow crystals: mp 65–72 °C; $^{31}P\{^1H\}$ NMR (C_6D_6) δ 22.5; IR (KBr) 2907, 2070, 1729, 1650, 1616, 1481, 1435, 1172, 1096, 540 cm^{-1}. Satisfactory elemental analysis could not be obtained even on multiply recrystallized samples; our best attempt gave the following. Anal. Calcd for $C_{34}H_{38}IrO_4P$: C, 55.64; H, 5.23. Found: C, 56.47; H, 5.17. FAB-MS (sulfolane): m/e 735/733, $(MH)^+$ ($^{193}Ir/^{191}Ir$).

Cp*IrPPh$_3$[OC(O)CH$_2$CH$_2$CO$_2$Et](H) (7b). A solution of succinic anhydride (10.5 mg, 1.05 × 10^{-1} mmol) in 5 mL of THF was added dropwise to a stirring yellow solution of **3** (63 mg, 9.92 × 10^{-2} mmol) in 10 mL of THF. The mixture was stirred for an additional 1 h and then concentrated in vacuo to a volume of ~1 mL. Pentane (~5 mL) was added, and the solution was cooled to −40 °C to yield 45 mg (62%) of yellow crystals of **7b**, which were washed with cold pentane: $^{31}P\{^1H\}$ NMR (C_6D_6) δ 22.5; IR (KBr) 2910, 2079, 1734, 1720, 1630, 1436, 1097, 697 cm^{-1}. Anal. Calcd for $C_{34}H_{40}IrO_4P$: C, 55.49; H, 5.49. Found: C, 55.65; H, 5.78. FAB-MS (sulfolane): m/e 735/733, $(M-H)^+$ ($^{193}Ir/^{191}Ir$).

Cp*IrPPh$_3$(NHPh)(H) (8a). Aniline (256 mg, 2.75 mmol), precooled to −40 °C, was added dropwise to a stirred yellow solution of **3** (256 mg, 0.403 mmol) in 20 mL of toluene. The solution was stirred for an additional 2 h. The solvent was removed under high vacuum to yield a yellow solid, which was triturated with 2 mL of pentane to afford a yellow powder (234 mg, 85%). Residual aniline was removed by dissolving the powder in benzene and removing the volatile materials by lyophilization: mp 178–180 °C dec; $^{31}P\{^1H\}$ NMR (C_6D_6) δ 13.8; $^{31}P\{^1H\}$ NMR (THF-d_8) δ 14.0; IR (KBr) 3357, 2907, 2128, 1486, 1436, 1094, 540 cm^{-1}; IR (Nujol mull) 3355, 2125 cm^{-1}. Anal. Calcd for $C_{34}H_{37}IrNP$: C, 59.80; H, 5.47; N, 2.05. Found: C, 60.03; H, 5.63; N, 1.92. FAB-MS (sulfolane): m/e 684/682, $(MH)^+$ ($^{193}Ir/^{191}Ir$).

The labeled analogues Cp*IrPPh$_3$(NDPh)(H) (**8a**-*N*-d_1) and Cp*IrPPh$_3$(^{15}NHPh)(H) (**8a**-^{15}N) were prepared from **3** and the appropriate labeled aniline, while Cp*IrPPh$_3$(NHPh)(D) (**8a**-*Ir*-d_1) was synthesized from Cp*IrPPh$_3$(OCD$_2$CD$_3$)(D) (**3**-d_6) and aniline. Selected spectral data for the labeled compounds: **8a**-*N*-d_1 IR

(KBr) 2492 cm^{-1} (N–D); **8a**-^{15}N ^1H NMR (THF-d_8) δ 1.24 (dd, J_{PH} = 4.5 Hz, J_{NH} = 75 Hz, ^{15}NH); **8a**-*Ir*-d_1 IR (KBr) 1530 cm^{-1} (Ir–D). In separate experiments, **8a**-*N*-d_1 and **8a**-*Ir*-d_1 were heated in C_6D_6 for 1 day for 45 °C. No scrambling of the deuterium occurred according to ^1H NMR or IR spectroscopy.

Cp*IrPPh$_3$(NHCH$_2$Ph)(H) (8b). Benzylamine (200 mg, 1.86 mmol) in 3 mL of toluene was added to a stirred yellow solution of **3** (120 mg, 0.189 mmol) in 5 mL of toluene. After 30 min the solvent was removed. Analysis of the residual yellow oil by ^1H NMR spectroscopy revealed a 10:1 ratio of product to starting material. An additional 100 mg of benzylamine (0.93 mmol) was added to a toluene solution of this mixture; removal of the solvents under high vacuum after another 30 min gave an orange-yellow oil. Repeated trituration with pentane gave **8b** as a yellow powder; concentration of the pentane solution gave additional crops of the light- and heat-sensitive powder (106 mg, 80%). Residual amine was removed by dissolution of the powder in benzene and lyophilization under high vacuum: mp 60 °C dec; $^{31}P\{^1H\}$ NMR (C_6D_6) δ 27.7; IR (KBr) 3282, 3054, 2919, 2080, 1435, 1096, 698 cm^{-1}. Anal. Calcd for $C_{35}H_{39}IrNP$: C, 60.32; H, 5.65; N, 2.01. Found: C, 61.26; H, 6.23; N, 1.97. Correct analyses could not be obtained despite several attempts; the compound appears to decompose at ambient temperature in the solid state. FAB-MS (sulfolane): *m/e* 697/695, $(M)^+$ ($^{193}Ir/^{191}Ir$).

Reaction of Cp*IrPPh$_3$(OEt)(H) with CO$_2$. A 20-mL cylindrical Pyrex vessel equipped with a vacuum stopcock and ground glass joint was charged with **3** (124 mg, 1.94×10^{-1} mmol) and 10 mL of benzene. The yellow solution was degassed by three freeze–pump–thaw cycles and treated with 10 atm of carbon dioxide (536 Torr in a 141.23-mL bulb). After 12 h the volatile components were removed under vacuum and 1 mL of C_6D_6 was added. A ^1H NMR spectrum showed, by integration, a mixture of Cp*IrPPh$_3$(OCO$_2$CH$_2$CH$_3$)(H) (**9**), Cp*IrPPh$_3$H$_2$ (**3**), and an unknown material in relative ratio 20:10:1:8. Attempts at obtaining pure samples of Cp*IrPPh$_3$(OCO$_2$CH$_2$CH$_3$)(H) (**9**) by crystallization, chromatography, or sublimation were unsuccessful. IR (C_6D_6): 2040, 1662, 1480, 1435, 1365, 1280, 1100, 1075, 700 cm^{-1}.

Cp*IrPPh$_3$(S$_2$COCH$_2$CH$_3$)(H) (10). Carbon disulfide (20 mL) was added via cannula to a Schlenk flask containing **3** (130 mg, 2.05×10^{-1} mmol). After stirring for 1 h, the solvent was removed under vacuum. Recrystallization from toluene/pentane at −40 °C gave yellow microcrystals of **10** (50.3 mg, 35%): mp 78–81 °C dec; $^{31}P\{^1H\}$ NMR (C_6D_6) δ 14.2; IR (C_6D_6) 2085, 1525, 1440, 1370, 1265, 1185, 1110, 1050, 815, 750, 700 cm^{-1}. High-resolution mass spectrum (EI) calcd for $C_{31}H_{36}IrOPS_2$: *m/e* 712.1574/710.1551, $(M)^+$ ($^{193}Ir/^{191}Ir$). Found: *m/e* 712.1590/710.1542, $(M)^+$ ($^{193}Ir/^{191}Ir$, deviation = 2.3/−1.2 ppm).

Cp*IrPPh$_3$(RNCO$_2$Et)(H) (11a–c). 11a (R = Ph). Phenyl isocyanate (25 μL, 0.230 mmol) was added to a benzene solution (25 mL) of **3** (75 mg, 0.118 mmol) and the mixture stirred for 1.5 h at 15 °C. The solvent and excess isocyanate were removed in vacuo to afford a yellow solid, which was recrystallized from toluene/pentane to give 72 mg of pure **11a** (80%): mp 119–120 °C dec; $^{31}P\{^1H\}$ NMR (C_6D_6) δ 16.3; IR (KBr) 2136, 1643 cm^{-1}. Anal. Calcd for $C_{37}H_{41}IrO_2PN$: C, 58.89; H, 5.43; N, 1.86. Found: C, 59.57; H, 5.47; N, 1.79. FAB-MS (sulfolane) *m/e* 754, $(M - H)^+$. This compound gave unsatisfactory analyses, but the *p*-tolyl analogue **11b** analyzes correctly.

11b (R = *p*-Tolyl). *p*-Tolyl isocyanate (75 μL, 0.59 mmol) was added to a solution of **3** (150 mg, 0.236 mmol) in 30 mL of toluene and the solution stirred for 6 h at 15 °C. The solution was concentrated; addition of hexamethyldisiloxane followed by cooling to −40 °C caused the precipitation of a yellow powder. The powder was redissolved in benzene, and the solvent and other volatile impurities were removed in vacuo to afford 105 mg (56%) of pure **11b**: mp 155–160 °C dec; $^{31}P\{^1H\}$ NMR (C_6D_6) δ 16.5; IR (KBr) 2139, 1641 cm^{-1}. Anal. Calcd for $C_{38}H_{43}IrO_2PN$: C, 59.38; H, 5.60; N, 1.82. Found: C, 59.43; H, 5.54; N, 1.86. FAB-MS (sulfolane) *m/e* 768, $(M - H)^+$.

Generation and Attempted Isolation of 11c (R = Me). Methyl isocyanate (375 Torr in a 27.55-mL bulb, 0.556 mmol) was vacuum-transferred into a flask containing **3** (150 mg, 0.236 mmol) in toluene (35 mL). The solution was stirred overnight at 25 °C. The toluene and excess isocyanate were removed in vacuo, and the resulting orange-brown oil was redissolved in benzene. The volatile materials were again removed in vacuo, yielding yellow powder (151 mg, 92%). A ^1H NMR spectrum showed a mixture of **11c**, Cp*IrPPh$_3$IrH$_2$, and two unknown hydrides in relative ratio 11:1:1:1, by integration. Attempts to isolate **11c** by recrystallization from pentane/toluene or from pentane/hexamethyldisiloxane were unsuccessful.

Cp*IrPPh$_3$[SC(S)NHPh](H) (12a). The anilide complex **8a** (45 mg, 6.59×10^{-2} mmol) was dissolved in a mixture of 20 mL of hexane and 5 mL of THF. Carbon disulfide (200 Torr in a 66.34-mL bulb, 0.712 mmol) was condensed into the flask at −196 °C. After thawing, the yellow solution was stirred overnight, causing an orange-yellow powder to fall out of solution. The solution was placed under vacuum briefly to remove excess carbon disulfide (reduction in volume of ~1 mL) and the powder was collected on a fine frit and washed with hexane (35 mg, 70%): mp 210 °C dec; $^{31}P\{^1H\}$ NMR (C_6D_6) δ 8.8; IR (KBr) 2077, 1653, 1521, 1496, 1436, 1285, 1095, 1028, 957 cm^{-1}; IR (Nujol mull) 2040, 1653, 1559, 1521, 1507, 1437, 1288, 1094, 1029, 955 cm^{-1}. Anal. Calcd for $C_{35}H_{37}IrNPS_2$: C, 55.38; H, 4.92; N. 1.85. Found: C, 54.78; H, 4.59; N, 1.50. The carbon value on this material was low despite several attempts at analysis. FAB-MS (sulfolane): *m/e* 759/757 and 760/758 (overlap of $(M)^+$ and $(MH)^+$ ($^{193}Ir/^{191}Ir$), 496/494, $(M - PPh_3H)^+$. The labeled analogues **Cp*Ir(PPh$_3$)[SC(S)NDPh](H) (12a-d_1)** and **Cp*Ir(PPh$_3$)[SC(S)^{15}NHPh](H) (12a-^{15}N)** were prepared from **8a**-*N*-d_1 and **8a**-^{15}N respectively. For **12a**-*N*-d_1: ^1H NMR (C_6D_6) the N–H signal at δ 11.2 was greatly reduced in intensity (~75%). For **12a**-^{15}N: ^1H NMR (C_6D_6) δ 11.20 (d, J_{NH} = 87 Hz).

Cp*IrPPh$_3$(SC(S)NHCH$_2$Ph)(H) (12b). Benzylamide complex **8b** (30 mg, 4.31×10^{-2} mmol) was dissolved in 15 mL of toluene. The yellow solution was freeze–pump–thawed and refrozen under vaccum, and carbon disulfide (36 Torr in a 66-mL bulb, 12.9×10^{-2} mmol) was condensed into the flask. On thawing, the solution became a lighter yellow. After stirring overnight, the volatile materials were removed in vacuo. The resulting light yellow solid was washed with 7 mL of pentane, in which it is sparingly soluble. The very pale yellow pentane solution was decanted and the solid dried in vacuo to afford 28 mg (85%) of yellow powder: mp 200–205 °C dec; $^{31}P\{^1H\}$ NMR (C_6D_6) δ 8.0; IR (KBr) 3222, 3055, 3027, 3002, 2913, 2089, 1490, 1482, 1453, 1435, 1094, 929, 697, 538 cm^{-1}. Anal. Calcd for $C_{36}H_{39}IrNPS_2$: C, 55.93; H, 5.10; N, 1.81. Found: C, 55.78; H, 5.31; N, 1.96. FAB-MS (sulfolane): *m/e* 774/772, 773/771, 772/770 (overlap of $(M)^+$, $(MH)^+$, and $(M - H)^+$ ($^{193}Ir/^{191}Ir$).

Cp*IrPPh$_3$(NPhC(O)NHMe)(H) (13b). Methyl isocyanate (40 Torr in a 66.34-mL bulb, 0.143 mmol) was condensed into a flask containing a frozen solution of anilido hydride complex **8a** (80 mg, 0.117 mmol) in 20 mL of toluene. The resulting yellow solution was stirred for 1.5 h. Removal of the solvent and excess isocyanate gave a yellow oil, which was recrystallized from toluene/pentane at −40 °C to give 58 mg (67%) of **13b** as a yellow solid: mp 95–100 °C dec; $^{31}P\{^1H\}$ NMR (C_6D_6) δ 16.3; IR (KBr) 3446, 3053, 3022, 2904, 2131, 1615, 1581, 1481, 1094, 696 cm^{-1}. Multiple analyses were uniformly low in carbon. Anal. Calcd for $C_{36}H_{40}IrN_2OP$: C, 58.43; H, 5.46; N, 3.79. Found: C, 56.16; H, 5.28; N, 3.26. FAB-MS (sulfolane): *m/e* 741/739, 740/738, 739/737 (overlapping peaks due to $(MH)^+$, $(M)^+$, and $(M - H)^+$.

Cp*IrPPh$_3$(CO) (14). Ethoxy hydride complex **3** (140 mg, 0.22 mmol) was dissolved in toluene (15 mL) in a glass bomb, which was then charged with 600 Torr of CO. Removal of the CO and solvent under reduced pressure after 1 day gave an orange residue, which was recrystallized from pentane at −40 °C to give 103 mg of orange-yellow solid (76%): $^{31}P\{^1H\}$ NMR (C_6D_6) δ 19.7; IR (C_6D_6) 1923, 1362 cm^{-1}. High-resolution mass spectrum (EI) calcd for $C_{29}H_{30}IrOP$: *m/e* 618.1663/616.1640, $(M)^+$ ($^{193}Ir/^{191}Ir$). Found: *m/e* 618.1652/616.1630 $(M)^+$ ($^{193}Ir/^{191}Ir$, deviation = −1.8/−1.6 ppm).

Cp*IrPPh$_3$(C$_2$H$_4$)[51] (15). Ethylene (67 Torr in a 141.23-mL bulb, 0.51 mmol) was condensed onto a frozen yellow solution of **3** (60 mg, 9.45×10^{-2} mmol) in 20 mL of toluene. Upon thawing, the solution turned orange. After 12 h the volatile materials were removed in vacuo to afford an orange solid, which was extracted with pentane; evaporation of the pentane yielded **15** as an orange

(51) Prepared independently in these laboratories: McGhee, W. D.; Bergman, R. G., unpublished results.

powder (46 mg, 79%): $^{31}P\{^1H\}$ NMR (C_6D_6) δ 19.6; IR (KBr) 2951, 2905, 1433, 1090, 697, 546 cm^{-1}. Anal. Calcd for $C_{30}H_{34}IrP$: C, 58.32; H, 5.56. Found: C, 58.61; H, 5.48. MS (EI): m/e 618/616, $(M)^+$ ($^{193}Ir/^{191}Ir$); 590/588, $(M - C_2H_4)^+$; 262 (base).

Cp*IrPPh$_3$(CN-*t*-Bu) (16). *Tert*-butyl isocyanide (19.7 Torr in a 141.23-mL bulb, 0.15 mmol), was vacuum-transferred into a flask containing **3** (75 mg, 0.118 mmol) in 30 mL of benzene. The solution turned orange upon thawing and was stirred overnight at 25 °C. Removal of the volatile materials in vacuo left a pure light orange solid (44 mg, 55%): mp 156–159 °C dec; $^{31}P\{^1H\}$ NMR (C_6D_6) δ 21.2; IR (KBr) 1872 cm^{-1}. Anal. Calcd for $C_{33}H_{39}IrPN$: C, 58.93; H, 5.80; N, 2.08. Found: C, 58.89; H, 5.93; N, 1.88. MS (EI): m/e 673, $(M)^+$. Analysis of the volatile materials by ^1H NMR spectroscopy confirmed the formation of ethanol.

Cp*Ir(PPh$_3$)$_2$ (17). Addition of triphenylphosphine (20.9 mg, 7.96×10^{-5} mol) to a yellow solution of **3** (50.6 mg, 7.96×10^{-5} mol) in 20 mL of benzene caused an immediate color change to deep red. After stirring for 1 h, removal of the volatile materials under vacuum and recrystallization from pentane at −40 °C gave red microcrystals (54.2 mg, 80%). Analysis of the volatile materials by gas chromatography confirmed the formation of ethanol. $^{31}P\{^1H\}$ NMR (C_6D_6): δ 20.7. $^{31}P\{^1H\}$ NMR (toluene-d_8): δ 20.1. IR (C_6D_6): 1360, 690 cm^{-1}. Anal. Calcd for $C_{46}H_{45}IrP_2$: C, 64.85; H, 5.32. Found: C, 64.70; H, 5.75. MS (EI): m/e 852, $(M)^+$; 277 (base).

Reaction of 3-d_1 with PPh$_3$ To Form Cp*Ir(PPh$_3$)$_2$ and EtOD. (a) Cp*IrPPh$_3$(OEt)(D) (3-d_1) (24 mg, 3.8×10^{-2} mmol) and a drop of toluene-d_8 were dissolved in C_6H_6, and the yellow solution was placed in an NMR tube. A ^2H NMR spectrum was recorded, showing peaks due to toluene-d_8 and Ir–D and a small peak due to ^2H incorporated in the C_5Me_5 during preparation of 3-d_1. PPh_3 (10 mg, 3.8×10^{-2} mmol) was added to the tube. The solution turned red within 5 min. Analysis of the ^2H NMR spectrum after 2 h showed formation of EtOD in 64% yield and no further incorporation of deuterium into the Cp* methyl groups. (b) Cp*IrPPh$_3$(OEt)(D) (200 mg, 0.314 mmol) and PPh_3 (83 mg, 0.32 mmol) were stirred in 10 mL of toluene for 1 h, at which time the solution was red. Tritylllithium (78 mg, 0.31 mmol) was added to the red solution. After 10 min, the solvent was removed in vacuo. Most of the Cp*Ir(PPh$_3$)$_2$ was destroyed by passing the reaction mixture down a column of alumina III and eluting with toluene. The remaining Ir was quenched by reaction with $HBF_4 \cdot Me_2O$ and filtration through silica. Removing solvent from the filtrate in vacuo gave 64 mg of white crystalline solid (85% yield of triphenylmethane). This material was recrystallized from pentane at −40 °C, leaving 26 mg of white crystals. Analysis by ^1H and ^2H NMR spectroscopy (ferrocene and toluene-d_8 internal standards) showed ~40% incorporation of deuterium into $Ph_3(CD(H)$.

[Cp*Ir(PPh$_3$)$_2$H]$^+$[BF$_4$]$^-$ (17a). Addition of $HBF_4 \cdot OEt_2$ (8.0 mg, 4.92×10^{-2} mmol) to a bright red ethereal (10 mL) solution of **17** (41.9 mg, 4.92×10^{-2} mmol) caused a white solid to precipitate. The white powder, pure **17a**, was collected on a frit and washed with ether (34.6 mg, 75%): ^1H NMR (acetone-d_6) δ 7.35 (m, 30 H), 1.46 (t, J_{HP} = 1.7 Hz, 15 H), −15.47 (t, J_{HP} = 27.8 Hz, 1 H); $^{13}C\{^1H\}$ NMR (acetone-d_6) δ 135.0 (m, virtual triplet, "J" = 5.1 Hz), 132.5 (m, virtual triplet, "J" = 30.2 Hz), 131.6, 129.0 (m, virtual triplet, "J" = 5.1 Hz), 100.8, 9.8; $^{31}P\{^1H\}$ NMR (acetone-d_6) δ 7.2, IR (silicone oil) 1944 cm^{-1} (broad). In several attempts, analyses gave low results for C. Anal. Calcd for $C_{46}H_{46}IrP_2BF_4$: C, 58.78; H, 4.94. Found: C, 56.56; H, 4.81. FAB-MS (thioglycerol/glycerol): m/e 853/851, $(M)^+$.

[Cp*Ir(PPh$_3$)$_2$D]$^+$[BF$_4$]$^-$ (17b). A solution of Cp*Ir(PPh$_3$)$_2$ (17) was prepared by the addition of PPh_3 (42 mg, 0.16 mmol) to Cp*IrPPh$_3$(OEt)(H) (100 mg, 0.157 mmol) in ether (10 mL). After 2.5 h D_2SO_4 (Aldrich, 98%) was added dropwise to the solution in the air, until the red color had bleached. The solvent was removed with a rotary evaporator and the yellow residue dissolved in aqueous methanol. $NaBF_4$ (190 mg, 1.73 mmol) was added; a white precipitate formed. The solvent was removed with a rotary evaporator. A CH_2Cl_2 solution of the pale yellow solid residue was layered with hexane and cooled to −40 °C. Removing the supernatant with a pipet gave a yellow oil, which under high vacuum became a yellow powder, yield 125 mg (93%). ^1H and ^2H NMR analysis in acetone-d_6 and acetone showed ~90% incorporation of D into the metal hydride position. The IR spectrum was essentially superimposable with that of **17a**, and no Ir–D stretch could be confidently assigned.

Deprotonation of 17a,b by Ethoxide To Give 17. (a) Addition of 1 mg of NaOEt (1.5×10^{-2} mmol) to a clear solution of **17a** in acetone (11 mg, 1.3×10^{-2} mmol) turned the solution red. The acetone was removed in vacuo and the red solid extracted with pentane. Removal of the pentane in vacuo gave a red oil, which was identified as Cp*Ir(PPh$_3$)$_2$ (17) by ^1H NMR spectroscopy. (b) Addition of sodium ethoxide (2 mg, 2.9×10^{-2} mmol) to a clear solution of 22 mg (2.6×10^{-2} mmol) of **17b** in acetone caused immediate formation of a red color. An identical workup gave a red oil, which was again identified as Cp*Ir(PPh$_3$)$_2$ (17) by its ^1H NMR spectrum. ^2H NMR analysis of this material showed that it contained no deuterium.

Cp*IrPPh$_3$(PPh$_2$Me) (18). Diphenylmethylphosphine (52 mg, 0.26 mmol) was added all at once as a solution in 2 mL of toluene to a yellow solution of ethoxy hydride complex **3** in 5 mL of toluene. The solution immediately turned orange-red. It was stirred for 2 h, at which time it was bright red. Removal of the solvent in vacuo gave a red oil. This was triturated with pentane (4 × 1 mL) to leave red microcrystals, which were readily separated from the supernatant by decantation and washed with cold pentane, yielding 154 mg (75%): $^{31}P\{^1H\}$ NMR (C_6D_6) δ 22.3 (d, J = 25.9 Hz, PPh_3), −6.4 (d, J = 25.9 Hz, PPh_2Me); IR (KBr) 2904, 1482, 1435, 1092, 884, 745, 720, 696, 545, 512 cm^{-1}. Anal. Calcd for $C_{41}H_{43}P_2Ir$: C, 62.33; H, 5.50. Found: C, 62.12; H, 5.24.

Cp*Ir(PAr$_3$)Cl$_2$ (Ar = *p*-XC$_6$H$_4$; X = F, Me, MeO) (19a–c). These compounds were prepared by the same procedure as the parent (X = H) complex, by refluxing $[Cp^*IrCl_2]_2$ with the triarylphosphine in ethanol overnight, and isolated by filtration.

a, X = F: 83%; mp >230 °C; ^1H NMR ($CDCl_3$) δ 7.69 (m, 6 H), 7.05 (m, 6 H), 1.34 (d, J = 2.1 Hz, 15 H); $^{13}C\{^1H\}$ NMR ($CDCl_3$) δ 164.0 (d, J_{CF} = 251 Hz, *C*F), 136.7 (m), 128.0, 115.2 (m), 92.9 (d, J = 2.4 Hz, C_5Me_5), 8.4 ($C_5\mathit{Me}_5$); $^{31}P\{^1H\}$ NMR ($CDCl_3$) δ −0.3; IR (KBr) 2921, 1590, 1499, 1163 cm^{-1}. Anal. Calcd for $C_{28}H_{27}IrCl_2PF_3$: C, 47.06; H, 3.82. Found: C, 47.11; H, 3.77. FAB-MS (nitrophenyloctyl ether): m/e 714/712, $(M)^+$ ($^{193}Ir/^{191}Ir$).

b, X = Me: 87%; mp >230 °C; ^1H NMR ($CDCl_3$) δ 7.59 (m, 6 H), 7.12 (m, 6 H), 2.32 (9 H), 1.33 (d, J = 2.1 Hz, 15 H); $^{13}C\{^1H\}$ NMR ($CDCl_3$) δ 140.2 (ipso $CH_3C_6H_4$), 135.0, 134.6 (d, J = 10.1 Hz, ortho or meta PC_6H_4), 128.4 (d, J = 10.6 Hz, ortho or meta PC_6H_4), 92.3 (d, J = 2.3 Hz, C_5Me_5), 21.3 ($C_6H_4CH_3$), 8.3 ($C_5\mathit{Me}_5$); $^{31}P\{^1H\}$ NMR ($CDCl_3$) δ 0.3; IR (KBr) 2917, 1563, 1500, 1098 cm^{-1}. Anal. Calcd for $C_{31}H_{36}IrCl_2P$: C, 52.98; H, 5.17. Found: C, 53.03; H, 5.13. FAB-MS (nitrophenyloctyl ether): m/e 702/700, $(M)^+$ ($^{193}Ir/^{191}Ir$).

c, X = MeO: 88%; mp >230 °C; ^1H NMR ($CDCl_3$) δ 7.61 (m, 6 H), 6.83 (m, 6 H), 3.77 (9 H), 1.33 (d, J = 2.0 Hz, 15 H); $^{13}C\{^1H\}$ NMR ($CDCl_3$) δ 160.1 ($COCH_3$), 136.1 (d, J = 10.8 Hz, ortho or meta PC_6H_4), 123.6, 113.2 (d, J = 11.0, ortho or meta PC_6H_4), 92.3 (C_5Me_5), 55.2 ($C_6H_4OCH_3$), 8.4 ($C_5\mathit{Me}_5$); $^{31}P\{^1H\}$ NMR ($CDCl_3$) δ −1.6; IR (KBr) 2915, 1595, 1502, 1254 cm^{-1}. Anal. Calcd for $C_{31}H_{36}IrCl_2PO_3$: C, 49.59; H, 4.84. Found: C, 49.53; H, 4.82. FAB-MS (nitrophenyloctyl ether): m/e 750/748, $(M)^+$ ($^{193}Ir/^{191}Ir$).

Cp*IrPAr$_3$(OEt)(H) (Ar = *p*-XC$_6$H$_4$; X = F, Me, MeO) (20a–c). These were synthesized as the parent (X = H, **3**), from the dichlorides (**19a–c**) with sodium ethoxide in ethanol.

a, X = F: ^1H NMR (C_6D_6) δ 7.57–7.45 (m, 6 H), 6.8–6.7 (m, 6 H), 3.75–3.40 (dm, 2 H), 1.50 (d, J = 1.9 Hz, 15 H), 1.06 (t, J = 6.8 Hz, 3 H), −13.44 (d, J = 37.8 Hz, 1 H); $^{13}C\{^1H\}$ NMR (C_6D_6) δ 164.1 (d, J_{CF} = 250 Hz, *C*F), 136.4 (m), 130.9 (dd, J_{PC} = 55.9 Hz, J_{CF} = 30 Hz, ipso *P*C), 114.9 (m), 91.9 (d, J = 3.3 Hz, C_5Me_5), 75.5 (OCH_2CH_3), 23.3 (OCH_2CH_3), 9.7 ($C_5\mathit{Me}_5$); $^{31}P\{^1H\}$ NMR (C_6D_6) δ 12.1; IR (KBr) 2073, 1590, 1496, 1095 cm^{-1}. Several attempts at analyses were unsuccessful. In this case some results gave high carbon values. Anal. Calcd for $C_{30}H_{33}IrOPF_3$: C, 52.22; H, 4.83. Found: C, 53.92; H, 4.92.

b, X = Me: mp 75–80 °C dec; ^1H NMR (C_6D_6) δ 7.78 (m, 6 H), 6.97 (m, 6 H), 3.81–3.62 (dm, 2 H), 2.04 (9 H), 1.66 (d, J = 1.3 Hz, 15 H), 1.14 (t, J = 6.6 Hz, 3 H); −13.27 (d, J = 38.0 Hz, 1 H); $^{13}C\{^1H\}$ NMR (C_6D_6) δ 139.2 ($C_6H_4CH_3$), 134.5 (d, J = 10.3 Hz, ortho or meta PC_6H_4), 133.0 (d, J_{PC} = 55.3 Hz, ipso *P*C), 128.5 (d, J = 10.3 Hz, ortho or meta PC_6H_4), 91.3 (C_5Me_5), 75.8 (OCH_2CH_3), 24.0 (OCH_2CH_3), 21.2 ($C_6H_4CH_3$), 9.8 ($C_5\mathit{Me}_5$); $^{31}P\{^1H\}$ NMR (C_6D_6) δ 13.8; IR (KBr) 2075, 1097, 808, 531 cm^{-1}. Anal.

Calcd for $C_{33}H_{42}IrOP$: C, 58.46; H, 6.26. Found: C, 58.75; H, 6.45.

c, X = MeO: mp 75–80 °C dec; ^1H NMR (C_6D_6) δ 7.84–7.77 (m, 6 H), 6.80–6.76 (m, 6 H), 3.92–3.67 (dm, 2 H), 3.23 (9 H), 1.67 (d, J = 2.0 Hz, 15 H), 1.22 (t, J = 6.7 Hz, 3 H), −13.31 (d, J = 37.9 Hz, 1 H); $^{13}C\{^1H\}$ NMR (C_6D_6) δ 161.0 ($C_6H_4OCH_3$), 135.9 (d, J = 11.8 Hz, ortho or meta PC_6H_4), 127.8 (d, J_{PC} = 58.4 Hz, ipso PC, obscured by solvent), 113.3 (d, J = 11.0 Hz, ortho or meta PC_6H_4), 91.3 (d, J = 3.4 Hz, C_5Me_5), 75.8 (OCH_2CH_3), 54.7 ($C_6H_4OCH_3$), 24.2 (OCH_2CH_3), 9.9 (C_5Me_5); $^{31}P\{^1H\}$ NMR (C_6D_6) δ 9.7; IR (KBr) 2063, 1595, 1500, 1099 cm^{-1}. Anal. Calcd for $C_{33}H_{42}IrO_4P$: C, 54.60; H, 5.84. Found: C, 54.96; H, 6.06.

Cp*Ir(PAr$_3$)PPh$_3$ (Ar = p-XC$_6$H$_4$; X = F, Me, MeO) (21a–c). These compounds were prepared from **3** and the appropriate triarylphosphine as with the synthesis of **17**. Like **17** they are red crystalline solids.

a, X = F: mp 180–190 °C; ^1H NMR (C_6D_6) δ 7.65–7.40 (m), 6.90 (m), 6.63 (m), 1.47 (d, J = 1.2 Hz, 15 H); $^{13}C\{^1H\}$ NMR (C_6D_6) δ 163.2 (d, J_{CF} = 249 Hz, CF), 139.1 (d, J = 47.8 Hz, ipso PC), 136.7 (m), 135.1 (d, J = 11.4 Hz), 134.6, 126.8 (d, J = 9.7 Hz), 113.6 (m), 93.2 (C_5Me_5), 10.6 (C_5Me_5); $^{31}P\{^1H\}$ NMR (C_6D_6) δ 20.4 (d, J = 21.9 Hz, PPh_3), 16.7 (d, J = 23 Hz, PAr_3); $^{31}P\{^1H\}$ NMR (toluene-d_8) δ 20.5 (d, J = 21.5 Hz), 16.6 (d, J = 21.5 Hz); IR (KBr) 1230, 1195, 1161, 1118, 1094 cm^{-1}. Anal. Calcd for $C_{46}H_{42}IrP_2F_3$: C, 60.98; H, 4.68. Found: C, 60.95; H, 4.70. FAB-MS (sulfolane): m/e 907/905, $(MH)^+$.

b, X = Me: mp 120 °C; ^1H NMR (C_6D_6) δ 7.8–7.6 (m), 7.0–6.9 (m), 6.80 (m), 2.04 (9 H), 1.62 (15 H); $^{13}C\{^1H\}$ NMR (C_6D_6) δ 140.1, 139.4, 137.6, 137.0, 136.4, 135.4 (d, J = 11.3 Hz), 127.5, 127.4 (obscured by solvent), 126.6 (d, J = 9.5 Hz), 93.0 (C_5Me_5), 21.1 ($C_6H_4CH_3$), 10.8 (C_5Me_5); $^{31}P\{^1H\}$ NMR (C_6D_6) δ 20.5 (d, J = 22.4 Hz), 17.3 (d, J = 22.4 Hz); $^{31}P\{^1H\}$ NMR (toluene-d_8) δ 20.5 (d, J = 22.5 Hz), 17.2 (d, J = 22.5 Hz); IR (KBr) 1192, 1118, 1094 cm^{-1}. Anal. Calcd for $C_{49}H_{51}IrP_2$: C, 65.82; H, 5.76. Found: C, 65.38; H, 5.76. FAB-MS (sulfolane): m/e 895/893, $(MH)^+$ ($^{193}Ir/^{191}Ir$).

c, X = MeO: ^1H NMR (C_6D_6) δ 7.74 (m), 7.1–6.9 (m), 6.64 (m), 3.27 (9 H), 1.63 (15 H); $^{13}C\{^1H\}$ NMR (C_6D_6) δ 159.0 ($COMe$), 139.8 (d, J = 46.8 Hz), 136.6 (d, J = 12.6 Hz), 135.3 (d, J = 11.2 Hz), 131.6 (d, J = 51.8 Hz), 126.6 (d, J = 9.6 Hz), 112.2 (d, J = 10.5 Hz), 93.0 (C_5Me_5), 54.7 ($C_6H_4OCH_3$), 10.9 (C_5Me_5); $^{31}P\{^1H\}$ NMR (C_6D_6) δ 21.0 (d, J = 22.5 Hz), 14.6 (d, J = 22.1 Hz); $^{31}P\{^1H\}$ NMR (toluene-d_8) δ 21.0 (d, J = 22.5 Hz), 14.6 (d, J = 22.5 Hz); IR (KBr) 1255, 1181, 1120, 1097 cm^{-1}. Anal. Calcd for $C_{49}H_{51}IrP_2O_3$: C, 62.46; H, 5.47. Found: C, 62.36; H, 5.62. FAB-MS (sulfolane): m/e 943/941, $(MH)^+$ ($^{193}Ir/^{191}Ir$).

Cp*Ir(PPh$_2$Me)$_2$ (22). A flask was charged with Cp*Ir(PPh$_2$Me)Cl$_2$ (338 mg, 0.565 mmol), NaOEt (102 mg, 1.50 mmol), and a stir bar. Ethanol (20 mL) was condensed into the flask and thawed. After 1.5 h of stirring, the orange slurry had turned yellow. The ethanol was removed in vacuo to given an orange oil. The oil was extracted with hexane, filtered to remove NaCl and excess NaOEt, concentrated, and cooled to −40 °C to give an orange oil, presumably Cp*Ir(PPh$_2$Me)(OEt)(H). To 293 mg (0.51 mmol) of this material in 10 mL of hexane was added PPh$_2$Me (105 mg, 0.525 mmol) in 5 mL of hexane. After 5 h the solvent was removed in vacuo from the orange solution to give a red oil. Trituration of this oil at ambient temperature with hexamethyldisiloxane left a red powder. Additional crops were obtained by concentration of the hexamethyldisiloxane solution for a total yield of 248 mg (67%): ^1H NMR (C_6D_6) δ 7.73–7.67 (m, 8 H), 7.18–7.03 (m, 12 H), 1.75 (d, J = 7.5 Hz), 1.69 (broad, 15 H); $^{31}P\{^1H\}$ NMR (C_6D_6) δ −5.5; $^{13}C\{^1H\}$ NMR (C_6D_6) δ 142.1–141.2 (5-line pattern, ipso PPh), 133.3 (broad), 128.3 (partially obscured by C_6D_6), 127.3 (broad), 92.3 (C_5Me_5), 23.2–22.4 (5-line pattern, PMe), 10.8 (C_5Me_5); IR (KBr) 3053, 2916, 1435, 1098, 879, 797, 513 cm^{-1}. Anal. Calcd for $C_{36}H_{41}IrP_2$: C, 59.40; H, 5.69. Found: C, 56.03; H, 5.49. Correct analysis for C could not be obtained even on red crystals formed on multiple recrystallization from pentane.

Acknowledgment. We are grateful to Dr. F. J. Hollander, Director of the UC Berkeley X-ray Diffraction Facility (CHEXRAY), for determining the structure of complex **6c**. We also acknowledge support of this research by the National Institutes of Health (Grant No. GM-25459). We thank Johnson-Matthey for a loan of $IrCl_3 \cdot 3H_2O$.

Supplementary Material Available: Tables of positional parameters and temperature factors for **6c** (4 pages); a listing of X-ray structural details for **6c** (20 pages). Ordering information is given on any current masthead page.

Mechanism of Ligand Substitution in an Iridium Amide Complex

David S. Glueck and Robert G. Bergman*

Department of Chemistry, University of California, Berkeley, California 94720

Received October 29, 1990

Reaction of Cp*IrPPh$_3$Cl$_2$ (Cp* = η^5-C$_5$Me$_5$) with methyllithium gave Cp*IrPPh$_3$Me$_2$ (**1a**), which yielded Cp*IrPPh$_3$(Me)(Cl) (**2a**) on treatment with anilinium hydrochloride. The reactions of complex **2a** with silver acetate, benzylmagnesium chloride, and lithium anilide gave Cp*IrPPh$_3$(Me)(OAc) (**3a**), Cp*IrPPh$_3$(Me)(CH$_2$Ph) (**4a**), and Cp*IrPPh$_3$(Me)(NHPh) (**5a**), respectively. Cp*IrPPh$_3$(Me)(OPh) (**6a**) was prepared from **2a** and sodium phenoxide or from **3a** and potassium phenoxide. Reaction of **2a** with sodium ethoxide in ethanol gave Cp*IrPPh$_3$(Me)(H) (**7a**). Treatment of **1a–6a** with PPh$_2$Me gave PPh$_3$ and the corresponding Cp*Ir(PPh$_2$Me)(Me)(X) compounds (X = Me, **1b**; X = Cl, **2b**; X = OAc, **3b**; X = CH$_2$Ph, **4b**; X = NHPh, **5b**; X = OPh, **6b**). Complexes **1b–6b** were prepared independently as for **1a–6a** via Cp*Ir(PPh$_2$Me)Cl$_2$. The rate of the reaction of **5a** and PPh$_2$Me to give PPh$_3$ and **5b** does not depend on [PPh$_2$Me]. On the basis of this result, the temperature dependence of the rate, and the lack of inhibition by PPh$_3$, **5a** is proposed to reversibly form the ring-slipped intermediate (η^3-C$_5$Me$_5$)IrPPh$_3$(Me)(NHPh) (**8**), which is stabilized by nitrogen lone pair to metal electron donation and trapped by PPh$_2$Me to give the observed products. The large rate differences in the ligand substitutions of **1a–6a** are rationalized in light of this mechanism.

Introduction

Until recently, alkoxide and amide complexes of the late transition metals were uncommon, and the properties of M–O and M–N bonds in such compounds were little investigated.[1] The reactivity of these bonds often depends dramatically on the other ligands in the coordination sphere of the metal complex. In the iridium alkoxide and

(1) For a review see: Bryndza, H. E.; Tam, W. *Chem. Rev.* **1988**, *88*, 1163.

0276-7333/91/2310-1479$02.50/0